

2

**AD-A234 446**



**AN ANISOTROPIC LAMINATED DAMPED  
PLATE THEORY**

David John Barrett  
Air Vehicle and Crew Systems Technology Department (Code 6043)  
NAVAL AIR DEVELOPMENT CENTER  
Warminster, PA 18974-5000

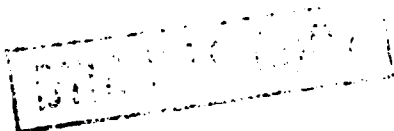
**30 JULY 1990**

PROGRESS REPORT  
Period Covering April 1989 To April 1990  
Task No. R0000101  
Work Unit No. HA642  
Program Element No. 61152N

*Approved for Public Release; Distribution is Unlimited.*

Prepared for  
Technical Director (Code 01)  
NAVAL AIR DEVELOPMENT CENTER  
Warminster, PA 18974-5000

DTIC  
ELECTE  
APR 30 1991  
S B D




91 4 30 048

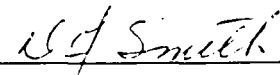
## NOTICES

**REPORT NUMBERING SYSTEM** — The numbering of technical project reports issued by the Naval Air Development Center is arranged for specific identification purposes. Each number consists of the Center acronym, the calendar year in which the number was assigned, the sequence number of the report within the specific calendar year, and the official 2-digit correspondence code of the Command Officer or the Functional Department responsible for the report. For example: Report No. NADC-88020-60 indicates the twentieth Center report for the year 1988 and prepared by the Air Vehicle and Crew Systems Technology Department. The numerical codes are as follows:

CODE	OFFICE OR DEPARTMENT
00	Commander, Naval Air Development Center
01	Technical Director, Naval Air Development Center
05	Computer Department
10	AntiSubmarine Warfare Systems Department
20	Tactical Air Systems Department
30	Warfare Systems Analysis Department
40	Communication Navigation Technology Department
50	Mission Avionics Technology Department
60	Air Vehicle & Crew Systems Technology Department
70	Systems & Software Technology Department
80	Engineering Support Group
90	Test & Evaluation Group

**PRODUCT ENDORSEMENT** — The discussion or instructions concerning commercial products herein do not constitute an endorsement by the Government nor do they convey or imply the license or right to use such products.

Reviewed By:  Date: 1/9/91  
Branch Head

Reviewed By:  Date: 1/10/91  
Division Head

Approved By:  Date: 1/11/91  
Director/Deputy Director

Unclassified

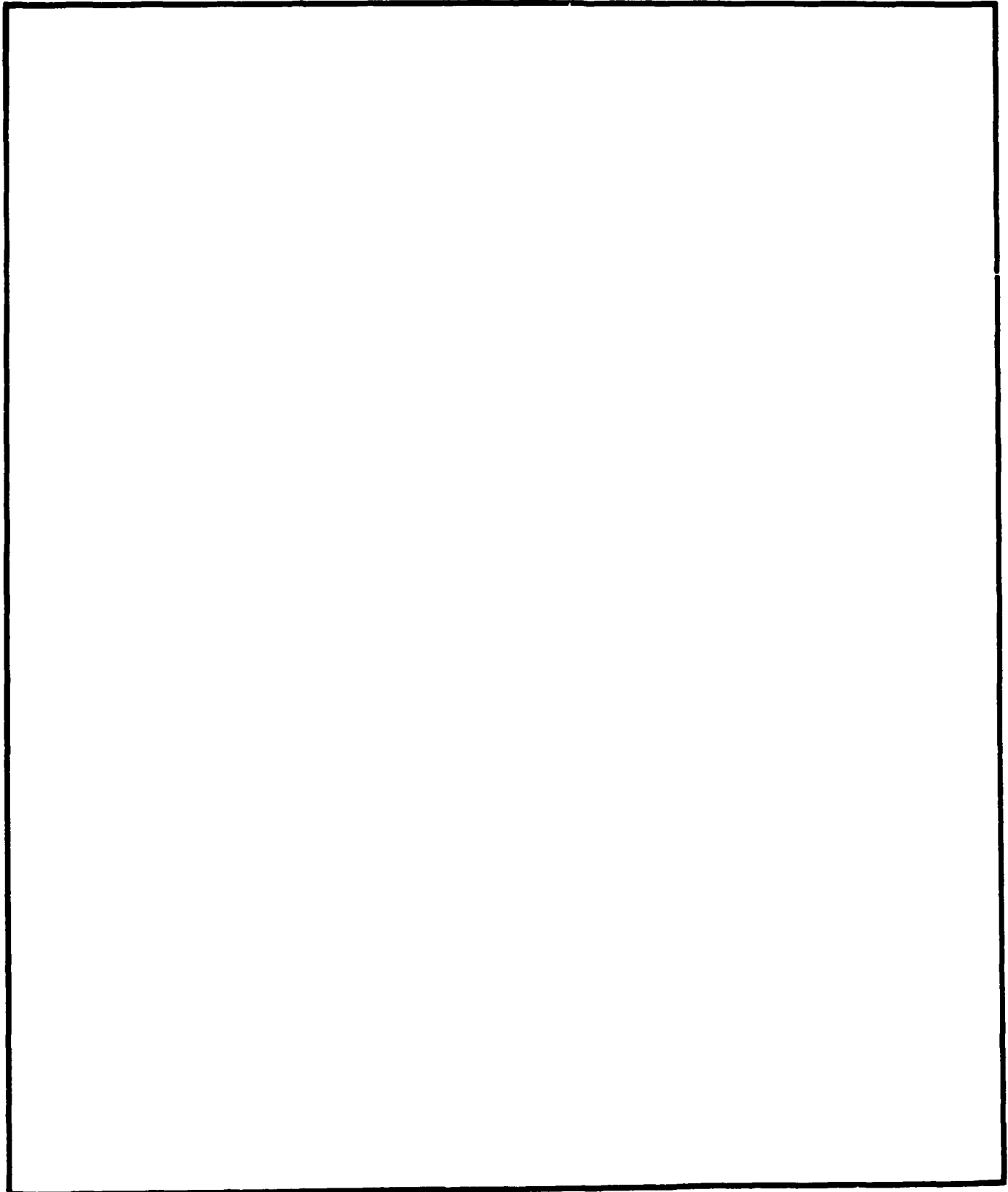
SECURITY CLASSIFICATION OF THIS PAGE

## REPORT DOCUMENTATION PAGE

Form Approved  
OMB No 0704-0188

1a REPORT SECURITY CLASSIFICATION <b>Unclassified</b>			1b RESTRICTIVE MARKINGS		
2a SECURITY CLASSIFICATION AUTHORITY			3 DISTRIBUTION AVAILABILITY OF REPORT <b>Approved for Public Release;</b>		
2b DECLASSIFICATION/DOWNGRADING SCHEDULE			Distribution is Unlimited		
4 PERFORMING ORGANIZATION REPORT NUMBER(S) <b>NADC-90066-60</b>			5 MONITORING ORGANIZATION REPORT NUMBER(S)		
6a NAME OF PERFORMING ORGANIZATION <b>Air Vehicle and Crew Systems Technology Department</b>		6b OFFICE SYMBOL (If applicable) <b>6043</b>	7a NAME OF MONITORING ORGANIZATION		
6c ADDRESS (City, State, and ZIP Code) <b>NAVAL AIR DEVELOPMENT CENTER WARMINSTER, PA 18974-5000</b>			7b ADDRESS (City, State, and ZIP Code)		
8a NAME OF FUNDING/SPONSORING ORGANIZATION <b>Technical Director</b>		8b OFFICE SYMBOL (If applicable) <b>01</b>	9 PROCUREMENT INSTRUMENT IDENTIFICATION NUMBER		
8c ADDRESS (City, State, and ZIP Code) <b>NAVAL AIR DEVELOPMENT CENTER Warminster, PA 18974-5000</b>			10 SOURCE OF FUNDING NUMBERS		
			PROGRAM ELEMENT NO <b>61152N</b>	PROJECT NO	TASK NO <b>R0000101</b>
					ACQUISITION NO <b>HA642</b>
11 TITLE (Include Security Classification) <b>An Anisotropic Laminated Damped Plate Theory</b>					
12 PERSONAL AUTHOR(S) <b>David John Barrett</b>					
13a TYPE OF REPORT <b>Progress</b>		13b TIME COVERED FROM <b>4/89</b> TO <b>4/90</b>		14 DATE OF REPORT (Year, Month, Day) <b>1990 July 30</b>	
				15 PAGE COUNT <b>43</b>	
16 SUPPLEMENTARY NOTATION					
17 COSAT CODES			18 SUBJECT TERMS (Continue on reverse if necessary and identify by block number)		
FIELD	GROUP	SUB-GROUP	<b>Structural Damping, Noise And Vibration Control, Structural Dynamics, Composite Structures</b>		
<b>01</b>	<b>03</b>				
<b>22</b>	<b>02</b>				
19 ABSTRACT (Continue on reverse if necessary and identify by block number) <p>This report describes the formulation of a structural theory for the analysis of laminated anisotropic damped plates. The plates consist of laminated face sheets sandwiching a single damping layer. The displacement degrees of freedom used to construct the analytical model are a generalization of those found in constrained layer theory. Variational principles are used to form the equations of motion which are solved for the steady state response of simply supported semi-infinite plates. The analysis is used to examine the effect of stress coupling and compliant layering on improving the dynamic resistance of damped structures loaded in flexure.</p>					
20 DISTRIBUTION AVAILABILITY OF ABSTRACT <input type="checkbox"/> UNCLASSIFIED UNLIMITED <input checked="" type="checkbox"/> SAME AS RPT <input type="checkbox"/> DTIC USERS			21 ABSTRACT SECURITY CLASSIFICATION <b>Unclassified</b>		
22a NAME OF RESPONSIBLE INDIVIDUAL <b>David John Barrett</b>			22b TELEPHONE (Include Area Code) <b>215-441-3770</b>		22c OFFICE SYMBOL <b>6043</b>

SECURITY CLASSIFICATION OF THIS PAGE



DD Form 1473, JUN 86 (Reverse)

SECURITY CLASSIFICATION OF THIS PAGE

CONTENTS

	Page
Figures .....	iv
Tables .....	iv
1.0 Introduction .....	1
1.1 Purpose .....	1
1.2 Background .....	1
2.0 Theory of Anisotropic Laminated Damped Plates .....	3
2.1 Analytical Model .....	3
2.2 Theoretical Development .....	5
3.0 Semi-Infinite Simply Supported Plates .....	15
3.1 Structural Description .....	15
3.2 Solution .....	16
3.3 Analytical Approach .....	18
4.0 Applications .....	19
4.1 Problem Description .....	19
4.2 Numerical Results .....	22
5.0 Conclusions .....	33
6.0 References .....	35
7.0 Nomenclature .....	37
Appendix A - Matrix Elements .....	A-1



<b>Accession For</b>	
NTIS GRA&I	<input checked="" type="checkbox"/>
DTIC TAB	<input type="checkbox"/>
Unannounced	<input type="checkbox"/>
Justification	
By	
Distribution/	
Availability Codes	
Dist	Avail and/or Special
A-1	

## NADC-90066-60

### FIGURES

Figure		Page
1	Damped Plate Structure .....	4
2	The Displacement Degrees of Freedom .....	7
3	Material Properties of Scotchdamp SJ2015X, Type 112 @20°C .....	21
4	Modal Damping for Bending Modes 1 to 3 .....	23
5	Modal Damping for Bending Modes 1 to 3 .....	24
6	Modal Damping for Bending Modes 1 to 5 .....	26
7	Forced Center Deflection for Bending Modes 1 to 5 .....	27
8	Modal Damping vs the Modulus of the Compliant Layer .....	30
9	The Phase Lag of the Core Rotation vs the Modulus of the Compliant Layer .....	31

### TABLES

Table		Page
1	Material Properties of IM6-3501 Carbon-Epoxy .....	20
2	Optimized Modal Designs .....	29

## 1.0 Introduction

### 1.1 Purpose

In this work a structural theory is devised for the analysis of laminated anisotropic damped plates. The plate consists of laminated face sheets sandwiching a single damping layer. The displacement degrees of freedom used to construct the analytical model are a generalization of those found in constrained layer theory. Variational principles are used to form the equations of motion which are solved for the steady state excitation of simply supported semi-infinite plates. The purpose for developing such an analytical model is to provide a tool for examining the effects of stress coupling and compliant layering in improving the performance of damped structures loaded in flexure.

### 1.2 Background

Highly damped structure is built by combining stiffness and damping materials into a single structural form. An example of such a composite construction is a planar lamination of stiffness and damping layers. Under bending, the deformation of the stiffness layers shear the damping layers which, because of their viscosity, dissipate part of the strain energy. Thus, resonant vibrational responses are controlled by the conversion of vibrational energies into heat. Damped structures based on this principle include constrained layer treatments, sandwich constructions and damped plates [1,2]. In vibrational environments these composite components have operational characteristics, durability, and service life that far exceed that of components based solely on stiffness materials [3,4].

Any design approach that increases the rate or amount of straining in the damping materials of a composite construction has the potential of improving the structural damping. Towards this end, research has been devoted to examining the use of discontinuous stiffness layers in order to introduce favorable edge effects [5]. Also, designs have been investigated that increase the thickness deformation of the damping layers [6,7]. Additional design approaches can be

found in the use of anisotropy and lamination.

When anisotropic stiffness materials are incorporated into damped composite construction, a coupling between normal and shear effects (stress coupling) is created. Stress coupling produces components of strain in the damping layers that do not occur in isotropic designs while retaining and adding to those components that already do occur. Conceivably this increased straining of the damping material would lead to higher energy dissipation and improved structural performance.

Lamination can be used to favorably change the stiffnesses of a structure. For instance, consider a damped composite plate system with layered stiffness face sheets and a damping core. If the stiffness layers adjacent to the core are replaced by a material more compliant than the outer stiffness layers then the construction would have virtually unchanged bending stiffness but directly reduced in-plane facial extensional stiffness. Under transverse vibration, the axially compliant face sheets can increase the amount of relative in-plane motion between the face sheets, thereby leading to an increase in the rate of core straining and energy dissipation.

The pioneering work in the use of stress coupling to assist the control of dynamic responses examined the performance of sandwich constructions [8]. The results of this study were limited since the analytical model was based on displacement fields that were too elementary to fully characterize the deformational response of composite constructions with compliant damping layers. This shortcoming was rectified in a later work which examined stress coupling and lamination in damped bending elements [9]. An additional effort in this area studied the use of stress coupling to improve the damping of tension-compression members [10].

In the present work a lamination theory is formulated that is applicable to a general class of damped plate structures. The theory contains all of the elements necessary for examining the effects of anisotropy and lamination in constrained layer treatments, damped sandwiches, damped plates and other damping designs. The theory also includes all of the components of translational and rotational mass inertia plus Timoshenko shear theory.



## 2.0 The Theory of Anisotropic Laminated Damped Plates

## 2.1 Analytical Model

The damped plate structure consists of top and bottom face sheets sandwiching a single damping layer (see Figure 1). The face sheets are layered with a total of  $N^T$  layers in the top face sheet and  $N^B$  layers in the bottom face sheet. The thicknesses of the individual layers are designated by  $t_n^T$  for the top layers,  $t_n^B$  for the bottom layers and  $t^D$  for the damping layer. (Here the subscript  $n$  identifies individual stiffness layers while the superscripts T (top), D (damping), and B (bottom) refer to specific parts of the structure). The right handed global coordinate system shown in Figure 1 and used in the development consists of the coordinates  $x_1$  and  $x_2$ , which are located in the planar mid-surface of the damping layer (the reference surface), and the transverse coordinate  $x_3$ .

To analytically model the described structure the following assumptions are made:

1. The in-plane deformations of the face sheets vary linearly through the face sheet thickness;
2. The in-plane deformations of the damping layer vary linearly through it's thickness;
3. The in-plane displacement fields are continuous across the interfaces (perfect bonding);
4. The transverse displacement is the same for all parts of the cross section.
5. The moduli of all of the materials of construction can be treated by the Complex Modulus model;
6. The material model for the stiffness layers is transversely isotropic but neglects the thickness normal stresses. The axis of isotropy is parallel to the mid-surface;
7. The material model for the damping layer is isotropic but includes only shear stresses.

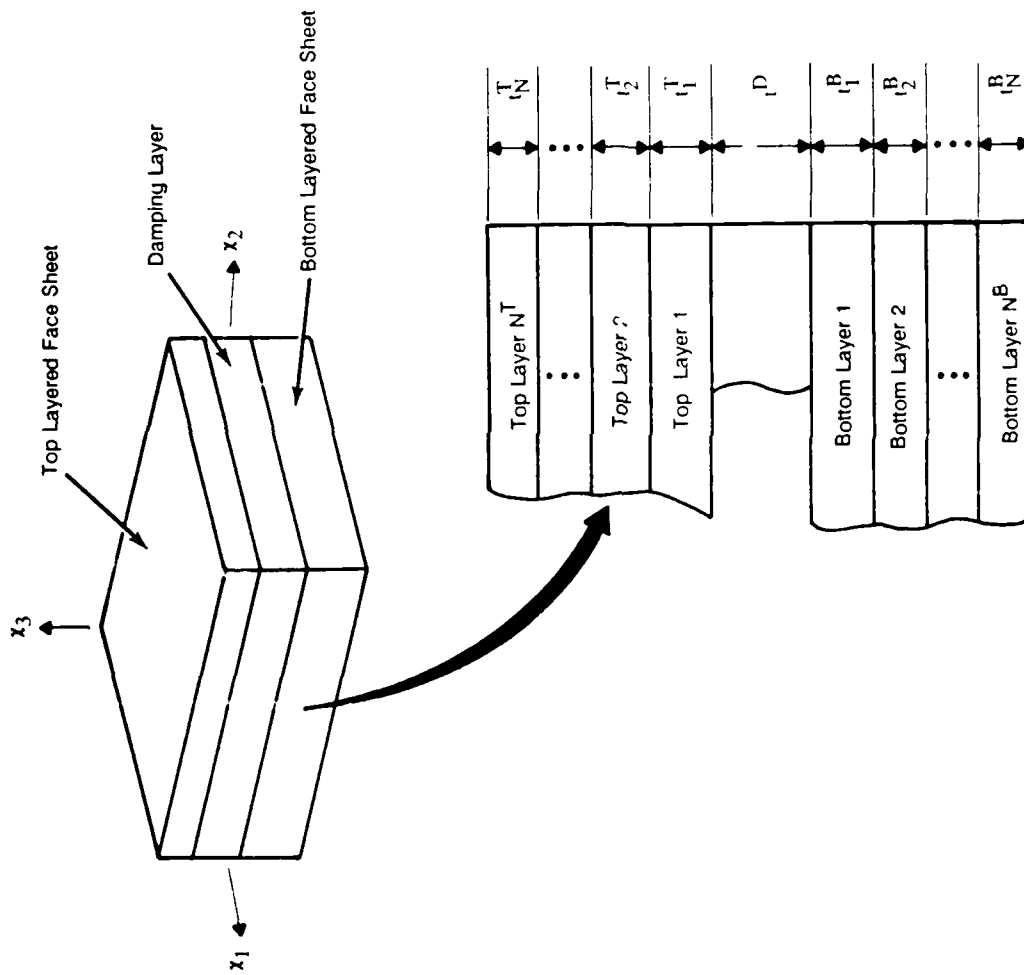


Figure 1. Damped Plate Structure

## 2.2 Theoretical Development

The equations of motion for the damped plate structure are derived by using Hamilton's Principle in conjunction with Reissner's Variational Theorem. Since Hamilton's Principle is only applicable to conservative systems, the material properties are initially treated as being purely elastic without any damping. The energy integrals are then formulated and minimized for this provisional, fully elastic system. Once the equations of motion and the force-displacement relations are derived, damping can be introduced by invoking the Correspondence Principle in which the elastic moduli are replaced by the complex viscoelastic moduli of the Complex Modulus model. Application of the damped plate model is therefore limited to steady state harmonic vibrations.

Through Hamilton's Principle the development proceeds by finding the motion that minimizes the integral

$$I = \int_{\tau_1}^{\tau_2} (K - R) d\tau \quad (2.2.1)$$

where  $K$  is the kinetic energy of the system and  $R$  is Reissner's Functional. The integration is over the time variable  $\tau$  between the instants of time  $\tau_1$  and  $\tau_2$ . The kinetic energy of the system is calculated from

$$K = \frac{1}{2} \int_V \rho \dot{u}_i \dot{u}_i dV \quad (2.2.2)$$

where  $\rho$  is the mass density,  $V$  is the volume and the  $u_i$  are the displacements. (Throughout this development an over dot will indicate differentiation with respect to time). Reissner's Functional for the structure is

$$R = \int_V (\sigma_{ij} \epsilon_{ij} - W(\sigma_{ij})) dV - \int_{S_T} T_i u_i dS \quad (2.2.3)$$

where  $\sigma_{ij}$  and  $\epsilon_{ij}$  are the stress and strain tensors,  $W(\sigma_{ij})$  is the strain energy density expressed in terms of the stresses, the  $T_i$  are the tractions, and  $S_T$  is that portion of the surface over which the tractions act.

The integrands of equations (2.2.2) and (2.2.3) are developed from the assumptions of the analytical model. Starting with assumptions 1 through 4, the motion of the structure is expressed in terms of nine unknown displacement degrees of freedom. Using these functions the displacement fields are found to be:

Top Face Sheet

$$u_1 = u_1^0(x_1, x_2, \tau) + \frac{1}{2}t^D \alpha_1^D(x_1, x_2, \tau) + (x_3 - \frac{1}{2}t^D) \alpha_1^T(x_1, x_2, \tau) \quad (2.2.4)$$

$$u_2 = u_2^0(x_1, x_2, \tau) + \frac{1}{2}t^D \alpha_2^D(x_1, x_2, \tau) + (x_3 - \frac{1}{2}t^D) \alpha_2^T(x_1, x_2, \tau) \quad (2.2.5)$$

$$u_3 = u_3^0(x_1, x_2, \tau) \quad (2.2.6)$$

Damping Layer

$$u_1 = u_1^0(x_1, x_2, \tau) + x_3 \alpha_1^D(x_1, x_2, \tau) \quad (2.2.7)$$

$$u_2 = u_2^0(x_1, x_2, \tau) + x_3 \alpha_2^D(x_1, x_2, \tau) \quad (2.2.8)$$

$$u_3 = u_3^0(x_1, x_2, \tau) \quad (2.2.9)$$

Bottom Face Sheet

$$u_1 = u_1^0(x_1, x_2, \tau) - \frac{1}{2}t^D \alpha_1^D(x_1, x_2, \tau) + (x_3 + \frac{1}{2}t^D) \alpha_1^B(x_1, x_2, \tau) \quad (2.2.10)$$

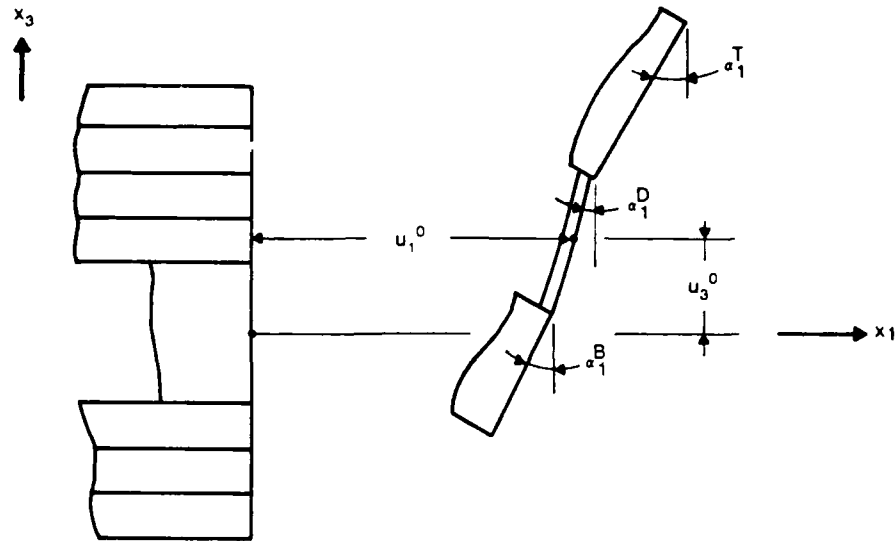
$$u_2 = u_2^0(x_1, x_2, \tau) - \frac{1}{2}t^D \alpha_2^D(x_1, x_2, \tau) + (x_3 + \frac{1}{2}t^D) \alpha_2^B(x_1, x_2, \tau) \quad (2.2.11)$$

$$u_3 = u_3^0(x_1, x_2, \tau) \quad (2.2.12)$$

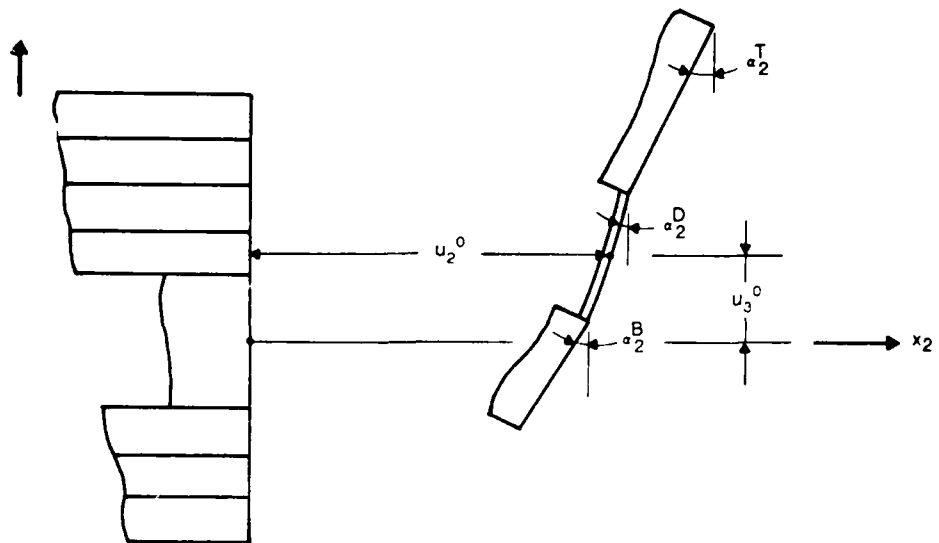
where the  $u_i^0$  are the reference surface displacements, the  $\alpha_i^D$  are the rotations of the damping layer about the reference surface, and the  $\alpha_i^T$  and  $\alpha_i^B$  are the rotations of the top and bottom face sheets (see Figure 2).

From the displacement fields, the strains in the reference surface and the plate curvatures are computed as

$$\epsilon_{ij}^0 = \frac{1}{2}(u_{i,j}^0 + u_{j,i}^0) \quad i, j = 1, 2 \quad (2.2.13)$$



Section Parallel to the  $x_1$  - Coordinate Line



Section Parallel to the  $x_2$  - Coordinate Line

Figure 2. The Displacement Degrees Of Freedom.

$$K_{ij}^T = \frac{1}{2}(\alpha_{ij}^T + \alpha_{ji}^T) \quad i, j=1, 2 \quad (2.2.14)$$

$$K_{ij}^D = \frac{1}{2}(\alpha_{ij}^D + \alpha_{ji}^D) \quad i, j=1, 2 \quad (2.2.15)$$

$$K_{ij}^B = \frac{1}{2}(\alpha_{ij}^B + \alpha_{ji}^B) \quad i, j=1, 2 \quad (2.2.16)$$

These expressions are combined to yield the following useful quantities

$$\bar{\epsilon}_{ij}^T = \epsilon_{ij}^0 + \frac{1}{2}t^D (K_{ij}^D - K_{ij}^T) \quad i, j=1, 2 \quad (2.2.17)$$

$$\bar{\epsilon}_{ij}^B = \epsilon_{ij}^0 - \frac{1}{2}t^D (K_{ij}^D - K_{ij}^B) \quad i, j=1, 2 \quad (2.2.18)$$

The strain fields are now computed as

Top Face Sheet

$$\epsilon_{ij} = \bar{\epsilon}_{ij}^T + x_3 K_{ij}^T \quad i, j=1, 2 \quad (2.2.19)$$

$$\epsilon_{i3} = \frac{1}{2}(\alpha_i^T + u_{3,i}^0) \quad i = 1, 2 \quad (2.2.20)$$

$$\epsilon_{33} = 0 \quad (2.2.21)$$

Damping Layer

$$\epsilon_{ij} = \bar{\epsilon}_{ij}^0 + x_3 K_{ij}^D \quad i, j=1, 2 \quad (2.2.22)$$

$$\epsilon_{i3} = \frac{1}{2}(\alpha_i^D + u_{3,i}^0) \quad i = 1, 2 \quad (2.2.23)$$

$$\epsilon_{33} = 0 \quad (2.2.24)$$

Bottom Face Sheet

$$\epsilon_{ij} = \bar{\epsilon}_{ij}^B + x_3 K_{ij}^B \quad i, j=1, 2 \quad (2.2.25)$$

$$\epsilon_{i3} = \frac{1}{2}(\alpha_i^B + u_{3,i}^0) \quad i = 1, 2 \quad (2.2.26)$$

$$\epsilon_{33} = 0 \quad (2.2.27)$$

Turning to assumption 6, the transversely isotropic constitutive relations for the stiffness layers are formed in the local layer coordinate system. Tensorial transformations are then used to reexpress these relations in the global  $x_1-x_2-x_3$  coordinate system. The matrix form of these expressions for the  $n$ 'th stiffness layer is

$$\begin{bmatrix} \sigma_{11}^n \\ \sigma_{22}^n \\ \sigma_{23}^n \\ \sigma_{13}^n \\ \sigma_{12}^n \end{bmatrix} = \begin{bmatrix} C_{1111}^n & C_{1122}^n & 0 & 0 & C_{1112}^n \\ C_{1122}^n & C_{2222}^n & 0 & 0 & C_{2212}^n \\ 0 & 0 & C_{2323}^n & C_{2312}^n & 0 \\ 0 & 0 & C_{2312}^n & C_{1212}^n & 0 \\ C_{1112}^n & C_{2212}^n & 0 & 0 & C_{1212}^n \end{bmatrix} \begin{bmatrix} \epsilon_{11} \\ \epsilon_{22} \\ 2\epsilon_{23} \\ 2\epsilon_{13} \\ 2\epsilon_{12} \end{bmatrix} \quad (2.2.28)$$

where the  $\sigma_{ij}^n$  are the layer stresses and the  $C_{ijkl}^n$  are the elastic constants. From assumption 7, the isotropic constitutive relation for the damping layer is

$$\begin{bmatrix} \sigma_{23} \\ \sigma_{13} \\ \sigma_{12} \end{bmatrix} = \begin{bmatrix} G & 0 & 0 \\ 0 & G & 0 \\ 0 & 0 & G \end{bmatrix} \begin{bmatrix} 2\epsilon_{23} \\ 2\epsilon_{13} \\ 2\epsilon_{12} \end{bmatrix} \quad (2.2.29)$$

where  $G$  is the shear modulus of the damping material.

To determine the layer stress resultants the constitutive relations are integrated over the layer thicknesses. The resulting expressions are then inverted to yield the following expressions

Top Layers

$$\sigma_{ij}^{nT} = \frac{H_3^{nT} F_{ij}^{nT} - H_2^{nT} M_{ij}^{nT}}{H^{nT}} + \frac{-H_2^{nT} F_{ij}^{nT} + H_1^{nT} M_{ij}^{nT}}{H^{nT}} x_3 \quad i, j = 1, 2 \quad (2.2.30)$$

$$\sigma_{i3}^{nT} = \frac{F_{i3}^{nT}}{t_n^T} \quad i = 1, 2 \quad (2.2.31)$$

Damping Layer

$$\sigma_{12}^D = \frac{F_{12}^D}{t^D} + \frac{12}{(t^D)^3} M_{12}^D x_3 \quad i, j = 1, 2 \quad (2.2.32)$$

$$\sigma_{i3}^D = \frac{F_{i3}^D}{t^D} \quad i = 1, 2 \quad (2.2.33)$$

Bottom Layers

$$\sigma_{ij}^{nB} = \frac{H_3^{nB} F_{ij}^{nB} - H_2^{nB} M_{ij}^{nB}}{H^{nB}} + \frac{-H_2^{nB} F_{ij}^{nB} + H_1^{nB} M_{ij}^{nB}}{H^{nB}} x_3 \quad i, j = 1, 2 \quad (2.2.34)$$

$$\sigma_{i3}^{nB} = \frac{F_{i3}^{nB}}{t_n^B} \quad i = 1, 2 \quad (2.2.35)$$

where the  $F_{ij}^{nT}$ ,  $F_{ij}^D$ , and  $F_{ij}^{nB}$  are the layer force stress resultants, the  $M_{ij}^{nT}$ ,  $M_{12}^D$ , and  $M_{ij}^{nB}$  are the layer moment stress resultants and the  $H_i^{nT}$  and  $H_i^{nB}$  are geometric quantities computed from

$$H_1^{nT} = t_n^T \quad (2.2.36)$$

$$H_2^{nT} = \frac{1}{2} H_1^{nT} (h_{n+1}^T + h_n^T) \quad (2.2.37)$$

$$H_3^{nT} = \frac{1}{3} H_1^{nT} ((h_{n+1}^T)^2 + h_n^T h_{n+1}^T + (h_n^T)^2) \quad (2.2.38)$$

$$H^{nT} = H_1^{nT} H_3^{nT} - H_2^{nT} H_2^{nT} \quad (2.2.39)$$

$$H_1^{nB} = t_n^B \quad (2.2.40)$$

$$H_2^{nB} = \frac{1}{2} H_1^{nB} (h_{n+1}^B + h_n^B) \quad (2.2.41)$$

$$H_3^{nB} = \frac{1}{3} H_1^{nB} ((h_{n+1}^B)^2 + h_n^B h_{n+1}^B + (h_n^B)^2) \quad (2.2.42)$$

$$H^{nB} = H_1^{nB} H_3^{nB} - H_2^{nB} H_2^{nB} \quad (2.2.43)$$

in which the  $h_n^T$  and  $h_{n+1}^T$  are the  $x_3$  coordinates of the bottom and top surfaces of the  $n$ 'th top layer and the  $h_n^B$  and  $h_{n+1}^B$  are the  $x_3$  coordinates of the top and bottom surfaces of the  $n$ 'th bottom layer.

The integrands of equations (2.2.2) and (2.2.3) are now computed using the expressions developed for the field variables. The stress resultants are included by performing the thickness integration of these integrals. The resulting expressions are then substituted into equation (2.2.1). Taking the variation of  $I$  with respect to the generalized displacements and forces and setting the coefficients of like variations to zero yields the governing system of differential



equations. These equations include the equations of motion, the force-displacement relations, and the boundary conditions (the initial conditions are irrelevant for the steady state problem).

Following this procedure the force-displacement equations are found to become

$$F_{ij}^{nT} = C_{ijkl}^{nT} (H_1^{nT} \epsilon_{kl}^T + H_2^{nT} K_{kl}^T) \quad i, j=1, 2; k, l=1, 2 \quad (2.2.44)$$

$$M_{ij}^{nT} = C_{ijkl}^{nT} (H_2^{nT} \epsilon_{kl}^T + H_3^{nT} K_{kl}^T) \quad i, j=1, 2; k, l=1, 2 \quad (2.2.45)$$

$$F_{ij}^{nB} = C_{ijkl}^{nB} (H_1^{nB} \epsilon_{kl}^B + H_2^{nB} K_{kl}^B) \quad i, j=1, 2; k, l=1, 2 \quad (2.2.46)$$

$$M_{ij}^{nB} = C_{ijkl}^{nB} (H_2^{nB} \epsilon_{kl}^B + H_3^{nB} K_{kl}^B) \quad i, j=1, 2; k, l=1, 2 \quad (2.2.47)$$

$$F_{i3}^{nT} = t_n^T C_{i3j3}^{nT} (\alpha_j^T + u_{3,j}^0) \quad i, j=1, 2 \quad (2.2.48)$$

$$F_{i3}^{nB} = t_n^B C_{i3j3}^{nB} (\alpha_j^B + u_{3,j}^0) \quad i, j=1, 2 \quad (2.2.49)$$

$$F_{12}^D = 2G t^D \epsilon_{12}^0 \quad (2.2.50)$$

$$M_{12}^D = \frac{1}{6} G (t^D)^3 K_{12}^D \quad (2.2.51)$$

$$F_{i3}^D = G t^M (\alpha_i^D + u_{3,i}^0) \quad i=1, 2 \quad (2.2.52)$$

Summing these expressions over the top and bottom face sheets leads to

Top Face Sheet

$$F_{ij}^T = A_{ijkl}^T u_{k,l}^0 + \frac{1}{2} t^D A_{ijkl}^T \alpha_{k,l}^D + (-\frac{1}{2} t^D A_{ijkl}^T + B_{ijkl}^T) \alpha_{k,l}^T \quad i, j=1, 2; k, l=1, 2 \quad (2.2.53)$$

$$F_{i3}^T = E_{ij}^T (\alpha_j^T + u_{3,j}^0) \quad i, j=1, 2 \quad (2.2.54)$$

$$M_{ij}^T = B_{ijkl}^T u_{k,l}^0 + \frac{1}{2} t^D B_{ijkl}^T \alpha_{k,l}^D + (-\frac{1}{2} t^D B_{ijkl}^T + D_{ijkl}^T) \alpha_{k,l}^T \quad i, j=1, 2; k, l=1, 2 \quad (2.2.55)$$

Bottom Face Sheet

$$F_{ij}^B = A_{ijkl}^B u_{k,l}^0 - \frac{1}{2} t^D A_{ijkl}^B \alpha_{k,l}^D + (\frac{1}{2} t^D A_{ijkl}^B + B_{ijkl}^B) \alpha_{k,l}^B \quad i, j=1, 2; k, l=1, 2 \quad (2.2.56)$$

$$F_{i3}^B = E_{ij}^B (\alpha_j^B + u_{3,j}^0) \quad i, j=1, 2 \quad (2.2.57)$$

$$M_{ij}^B = B_{ijkl}^B u_{k,l}^0 - \frac{1}{2} t^D B_{ijkl}^B \alpha_{k,l}^D + (\frac{1}{2} t^D B_{ijkl}^B + D_{ijkl}^B) \alpha_{k,l}^B \quad i, j=1, 2; k, l=1, 2 \quad (2.2.58)$$

where the  $F_{ij}^T$ ,  $F_{ij}^B$ ,  $M_{ij}^T$  and  $M_{ij}^B$  are the face sheet force and moment stress resultants and

$$A_{ijkl}^T = \sum_{n=1}^N C_{ijkl}^{nT} H_1^{nT} \quad i, j=1, 2; k, l=1, 2 \quad (2.2.59)$$

$$B_{ijkl}^T = \sum_{n=1}^N C_{ijkl}^{nT} H_2^{nT} \quad i, j=1, 2; k, l=1, 2 \quad (2.2.60)$$

$$D_{ijkl}^T = \sum_{n=1}^N C_{ijkl}^{nT} H_3^{nT} \quad i, j=1, 2; k, l=1, 2 \quad (2.2.61)$$

$$E_{ij}^T = \sum_{n=1}^N t_n^T C_{i3j3}^T \quad i, j=1, 2 \quad (2.2.62)$$

$$A_{ijkl}^B = \sum_{n=1}^M C_{ijkl}^{nB} H_1^{nB} \quad i, j=1, 2; k, l=1, 2 \quad (2.2.63)$$

$$B_{ijkl}^B = \sum_{n=1}^M C_{ijkl}^{nB} H_2^{nB} \quad i, j=1, 2; k, l=1, 2 \quad (2.2.64)$$

$$D_{ijkl}^B = \sum_{n=1}^M C_{ijkl}^{nB} H_3^{nB} \quad i, j=1, 2; k, l=1, 2 \quad (2.2.65)$$

$$E_{ij}^B = \sum_{n=1}^M t_n^B C_{i3j3}^B \quad i, j=1, 2 \quad (2.2.66)$$

Using equations 2.2.53 to 2.2.58 in the variational relations leads to the following form of the equations of motion

$$-F_{1jj}^T - F_{1jj}^B - F_{12,2}^D - P_1 + M\ddot{u}_1^0 + I_1^D \ddot{\alpha}_1^D + I_1^T \ddot{\alpha}_1^T + I_1^B \ddot{\alpha}_1^B = 0 \quad j=1, 2 \quad (2.2.67)$$

$$-F_{2jj}^T - F_{2jj}^B - F_{12,2}^D - P_2 + M\ddot{u}_2^0 + I_1^D \ddot{\alpha}_2^D + I_1^T \ddot{\alpha}_2^T + I_1^B \ddot{\alpha}_2^B = 0 \quad j=1, 2 \quad (2.2.68)$$

$$-F_{i3,i}^T - F_{i3,i}^B - F_{i3,i}^D - P_3 + M\ddot{u}_3^0 = 0 \quad i=1, 2 \quad (2.2.69)$$

$$\frac{1}{2} t^D (-F_{1jj}^T + F_{1jj}^B) + F_{13}^D - M_{12,2}^D + I_1^D \ddot{u}_1^0 + I_2^D \ddot{\alpha}_1^D + I_2^T \ddot{\alpha}_1^T + I_2^B \ddot{\alpha}_1^B = 0 \quad j=1, 2 \quad (2.2.70)$$

$$\frac{1}{2} t^D (-F_{2jj}^T + F_{2jj}^B) + F_{23}^D - M_{12,1}^D + I_1^D \ddot{u}_2^0 + I_2^D \ddot{\alpha}_2^D + I_2^T \ddot{\alpha}_2^T + I_2^B \ddot{\alpha}_2^B = 0 \quad j=1, 2 \quad (2.2.71)$$

$$\frac{1}{2} t^D F_{1jj}^T + F_{13}^T - M_{1jj}^T + I_1^T \ddot{u}_1^0 + I_2^T \ddot{\alpha}_1^D + I_3^T \ddot{\alpha}_1^T = 0 \quad j=1, 2 \quad (2.2.72)$$

$$\frac{1}{2}t^D F_{2jj}^T + F_{23}^T - M_{2jj}^T + I_1^T \ddot{u}_2^0 + I_2^T \ddot{\alpha}_2^D + I_3^T \ddot{\alpha}_2^T = 0 \quad j=1,2 \quad (2.2.73)$$

$$-\frac{1}{2}t^D F_{1jj}^B + F_{13}^B - M_{1jj}^B + I_1^B \ddot{u}_1^0 + I_2^B \ddot{\alpha}_1^D + I_3^B \ddot{\alpha}_1^B = 0 \quad j=1,2 \quad (2.2.74)$$

$$-\frac{1}{2}t^D F_{2jj}^B + F_{23}^B - M_{2jj}^B + I_1^B \ddot{u}_2^0 + I_2^B \ddot{\alpha}_2^D + I_3^B \ddot{\alpha}_2^B = 0 \quad j=1,2 \quad (2.2.75)$$

where the  $P_i$  are the applied tractions and the inertial constants are computed from

$$M^T = \sum_{n=1}^N \rho_n^T t_n^T \quad (2.2.76)$$

$$M^B = \sum_{n=1}^M \rho_n^B t_n^B \quad (2.2.77)$$

$$M = M^T + \rho^D t^D + M^B \quad (2.2.78)$$

$$I_1^T = \sum_{n=1}^N t_n^T \rho_n^T \left( \frac{h_{n+1}^T + h_n^T}{2} - \frac{1}{2} t^D \right) \quad (2.2.79)$$

$$I_1^D = \frac{1}{2} t^D (M^T - M^B) \quad (2.2.80)$$

$$I_1^B = \sum_{n=1}^M t_n^B \rho_n^B \left( \frac{h_{n+1}^B + h_n^B}{2} + \frac{1}{2} t^D \right) \quad (2.2.81)$$

$$I_2^T = \frac{1}{2} t^D I_1^T \quad (2.2.82)$$

$$I_2^D = \left( \frac{1}{2} t^D \right)^2 (M^T + M^B) + \rho^D \frac{(t^D)^3}{12} \quad (2.2.83)$$

$$I_2^B = -\frac{1}{2} t^D I_1^B \quad (2.2.84)$$

$$I_3^T = \sum_{n=1}^N \left( \left( \frac{1}{2} t^D \right)^2 \rho_n^T t_n^T - t^D \rho_n^T H_2^{nT} + \rho_n^T H_3^{nT} \right) \quad (2.2.85)$$

$$I_3^B = \sum_{n=1}^M \left( \left( \frac{1}{2} t^D \right)^2 \rho_n^B t_n^B + t^D \rho_n^B H_2^{nB} + \rho_n^B H_3^{nB} \right) \quad (2.2.86)$$

where  $\rho_n^T$  and  $\rho_n^B$  are the layer mass densities.

The natural boundary conditions are found to be

$$(F_{1j}^T n_j + F_{12}^D n_2 + F_{1j}^B n_j) \delta u_1^0 = 0 \quad j=1,2 \quad (2.2.87)$$

$$(F_{2j}^T n_j + F_{12}^D n_1 + F_{2j}^B n_j) \delta u_2^0 = 0 \quad j=1,2 \quad (2.2.88)$$

$$(F_{i3}^T n_i + F_{13}^D n_1 + F_{23}^D n_2 + F_{i3}^B n_i) \delta u_3^0 \quad i = 1,2 \quad (2.2.89)$$

$$\left(\frac{1}{2} t^D F_{1j}^T n_j + M_{12}^D n_2 - \frac{1}{2} t^D F_{1j}^B n_j\right) \delta \alpha_1^D = 0 \quad j=1,2 \quad (2.2.90)$$

$$\left(\frac{1}{2} t^D F_{2j}^T n_j + M_{12}^D n_1 - \frac{1}{2} t^D F_{2j}^B n_j\right) \delta \alpha_2^D = 0 \quad j=1,2 \quad (2.2.91)$$

$$\left(-\frac{1}{2} t^D F_{1j}^T n_j + M_{1j}^T n_j\right) \delta \alpha_1^T = 0 \quad j=1,2 \quad (2.2.92)$$

$$\left(-\frac{1}{2} t^D F_{2j}^T n_j + M_{2j}^T n_j\right) \delta \alpha_2^T = 0 \quad j=1,2 \quad (2.2.93)$$

$$\left(\frac{1}{2} t^D F_{1j}^B n_j + M_{1j}^B n_j\right) \delta \alpha_2^B = 0 \quad j=1,2 \quad (2.2.94)$$

$$\left(\frac{1}{2} t^D F_{2j}^B n_j + M_{2j}^B n_j\right) \delta \alpha_2^B = 0 \quad j=1,2 \quad (2.2.95)$$

where  $\delta$  is the variational symbol and the  $n_j$  are the direction cosines of the normals on the structural boundaries.

At this point the force-displacement relations are substituted into the equations of motion. This yields a set of nine displacement-equilibrium equations the unknowns of which are the nine functional displacement degrees of freedom. Solutions to specific problems are found by applying the appropriate set of boundary conditions and solving these displacement-equilibrium equations.

### 3.0 Semi-Infinite Simply Supported Plates

#### 3.1 Structural Description

The equations of the anisotropic laminated damped plate theory are extremely complex and are not readily solved by closed form or series solution methods. For instance, individual equations of the theory contain odd and even derivatives of the same spatial variable, which precludes a Fourier series solution. Semi-infinite simply supported plates, however, are an important class of problems for which a Fourier series solution can be found and in which stress coupling and lamination can be studied.

Consider a plate of finite length  $a$  in the  $x_1$  direction and of infinite extent in the  $x_2$  direction. On the  $x_1=0$  and  $x_1=a$  edges the plate is taken to be simply supported. Furthermore the applied loads on the plate are limited to be uniform in the  $x_2$  coordinate. For such a system all of the field variables are independent of the  $x_2$  coordinate, so that all of the differentiations with respect to this coordinate vanish. This simplifies the equations of motion which in matrix notation reduce to

$$[M][\ddot{u}] + [D][u] = [P] \quad (3.1.1)$$

where  $[M]$  is the mass matrix,  $[D]$  is a differential operator matrix,  $[u]$  is a vector of unknown displacement functions and  $[P]$  is a load vector. The elements of these matrices are given in Appendix A.

The natural boundary conditions for this structure reduce to the following edge conditions at  $x_1=0$  and  $x_1=a$

$$F_{11}^T = 0 \quad (3.1.2)$$

$$F_{11}^B = 0 \quad (3.1.3)$$

$$F_{12}^T + F_{12}^D + F_{12}^B = 0 \quad (3.1.4)$$

$$u_3^0 = 0 \quad (3.1.5)$$

$$\frac{1}{2}t^D F_{12}^T + M_{12}^D - \frac{1}{2}t^D F_{12}^B = 0 \quad (3.1.6)$$

$$M_{11}^T = 0 \quad (3.1.7)$$

$$M_{11}^B = 0 \quad (3.1.8)$$

$$-\frac{1}{2}t^D F_{12}^T + M_{12}^T = 0 \quad (3.1.9)$$

$$\frac{1}{2}t^D F_{12}^B + M_{12}^B = 0 \quad (3.1.10)$$

### 3.2 Solution

Equation (3.1.1) is solvable by the Fourier series method. To apply this method assume the following series expansions for the displacement degrees of freedom

$$u_1^0 = \sum_{m=1}^{\infty} U_1^m \cos\left(\frac{m\pi x_1}{a}\right) e^{i\Omega\tau} \quad (3.2.1)$$

$$u_2^0 = \sum_{m=1}^{\infty} U_2^m \cos\left(\frac{m\pi x_1}{a}\right) e^{i\Omega\tau} \quad (3.2.2)$$

$$u_3^0 = \sum_{m=1}^{\infty} U_3^m \sin\left(\frac{m\pi x_1}{a}\right) e^{i\Omega\tau} \quad (3.2.3)$$

$$\alpha_1^D = \sum_{m=1}^{\infty} A_1^{mD} \cos\left(\frac{m\pi x_1}{a}\right) e^{i\Omega\tau} \quad (3.2.4)$$

$$\alpha_2^D = \sum_{m=1}^{\infty} A_2^{mD} \cos\left(\frac{m\pi x_1}{a}\right) e^{i\Omega\tau} \quad (3.2.5)$$

$$\alpha_1^T = \sum_{m=1}^{\infty} A_1^{mT} \cos\left(\frac{m\pi x_1}{a}\right) e^{i\Omega\tau} \quad (3.2.6)$$

$$\alpha_2^T = \sum_{m=1}^{\infty} A_2^{mT} \cos\left(\frac{m\pi x_1}{a}\right) e^{i\Omega\tau} \quad (3.2.7)$$

$$\alpha_1^B = \sum_{m=1}^{\infty} A_1^{mB} \cos\left(\frac{m\pi x_1}{a}\right) e^{i\Omega\tau} \quad (3.2.8)$$

$$\alpha_2^B = \sum_{m=1}^{\infty} A_2^{mB} \cos\left(\frac{m\pi x_1}{a}\right) e^{i\Omega\tau} \quad (3.2.9)$$

where the superscripted constants are Fourier coefficients and  $\Omega$  is the frequency of the steady state excitation. It is easily shown that these expressions satisfy the boundary conditions.

The harmonically varying excitations (with respect to time) are also expressed in terms of Fourier series expansions

$$P_1(x_1, \tau) = \sum_{m=1}^{\infty} P_1^m \cos\left(\frac{m\pi x_1}{a}\right) e^{i\Omega\tau} \quad (3.2.10)$$

$$P_2(x_1, \tau) = \sum_{m=1}^{\infty} P_2^m \cos\left(\frac{m\pi x_1}{a}\right) e^{i\Omega\tau} \quad (3.2.11)$$

$$P_3(x_1, \tau) = \sum_{m=1}^{\infty} P_3^m \sin\left(\frac{m\pi x_1}{a}\right) e^{i\Omega\tau} \quad (3.2.12)$$

where the  $P_i^m$  are the Fourier coefficients determined from the Fourier formulae.

Substituting the above expansions into equation (3.1.1) results in an infinite number of uncoupled equations that can be grouped into sets by common indicial values. Thus a set of nine equations and nine unknowns is obtained for each indicial value where the unknowns of these equations are the Fourier coefficients of the displacement series. Expressing these equations in matrix form leads to the following general expression for each indicial value

$$-\Omega^2[M][U^m] + [B_m][U^m] = [P^m] \quad (3.2.13)$$

where  $[U^m]$  is a vector of Fourier displacement coefficients,  $[B_m]$  is a modal stiffness matrix whose elements are determined by the material and geometric properties of the structure, and  $[P^m]$  is a vector of the Fourier loading coefficients. The elements of these matrices are given in Appendix A.

The viscoelasticity of the original structure may now be introduced by invoking the Correspondence Principle. This is done by replacing the elastic material moduli with complex viscoelastic moduli. The elastic field variables are then reinterpreted as complex harmonic variables and, as assumed in the Fourier series expansion of the loadings, the excitation is limited

to steady state harmonic.

### 3.3 Analytical Approach

The analysis can be completed in several ways depending upon the type of information desired. For instance, the dynamic response of a damped plate to a specific excitation can be found through the direct solution of equations (3.2.13). The analysis begins by decomposing the spatial portion of the excitation into it's Fourier components. If necessary a suitable level of truncation is determined. Equations (3.2.13) are then formed and solved for each applicable indice. The displacement degrees of freedom are then synthesized from the Fourier expansions. Once the displacements are found, then any field variable of interest can be computed. If response spectrums are desired, the steps of this method are repeated throughout the frequency range of interest. Frequency dependent material properties are accounted for by updating their values at each step in the analysis.

If however, the modal loss factors are to be determined then the Damped Forced Vibration Mode Method [11] is applied. In general, high system damping is nonproportional so that there is a coupling between undamped normal modes, but a unique value of modal damping can still be found by considering a special case of forced vibration. In particular, consider harmonic loads that are proportional to the local mass inertia forces and that are in phase with the local velocity. Then

$$[P^m] = -i \eta \Omega^2 [M] [U^m] \quad (3.3.1)$$

For this loading Equation (3.2.13) becomes

$$[B_m] [U^m] - \Omega^2 (1 + \eta) [M] [U^m] = [0] \quad (3.3.2)$$

which can be rearranged into the form of a complex eigenvalue problem

$$[[B_m] - \Omega^2 (1 + i \eta) [M]] [U^m] = [0] \quad (3.3.3)$$

From this last equation the natural frequencies, loss factors, and complex mode shapes are extracted.



## 4.0 Applications

### 4.1 Structural Description

The semi-infinite damped plate examined in this analytical study has a width of 25.4 cm. The top and bottom face sheets of the plate consist of 6 stiffness layers with each layer having a thickness of 0.1/25 mm. The damping layer has a thickness of .0965 mm. The stiffness layers consist of IM6-3501 carbon-epoxy with a fiber volume fraction of 60%. The properties of this material are shown in Table 1 where the frequency dependence of the properties are neglected since the overall structural damping is dominated by the damping layer. The damping layer consists of Type 112 Scotchdamp SJ2015x. The frequency dependence of the moduli of this material are accounted for in the analysis. A plot of these properties is shown in Figure 3. The mass density of the damping material is .98 gm/cc.

To study the effects of stress coupling and compliant layering on structural damping, the fiber reinforced layers adjacent to the damping layer are given off-axis orientations with respect to the  $x_1$  coordinate direction. This arrangement of layers retains static stiffness by keeping the fibers in the outer plies oriented along the plate width. However, with off-axis orientations for the inner layers, the top and bottom face sheets can individually be unbalanced and unsymmetrical leading to full coupling effects (extensional-shear, extensional-bending/twisting and bending-twisting). Also, the off-axis orientation makes the inner layers more compliant with respect to the  $x_1$  coordinate direction. When the face sheets are bonded together by the damping layer the overall structural coupling is enhanced or diminished depending upon the layer orientations and the stiffness of the damping layer. For instance, with stiff damping layers the Love-Kirchoff hypothesis is valid so that the structural coupling of the damped plate is identical to that predicted by lamination theory. However, for flexible damping materials the top and bottom face sheets are not constrained to act in unison so that more complicated coupling phenomena can occur.

## NADC-90066-60

Table 1. Material Properties Of IM6-3501 Carbon-Epoxy.

Axial Extensional Modulus	148.GPa (21.5 Ms1)
Transverse Extensional Modulus	8.96 GPa (1.30 Ms1)
Axial Poisson's Ratio	.35
Axial Shear Modulus	4.48 GPa (0.65 Ms1)
Transverse Shear Modulus	2.07 GPa (0.30 Ms1)
Axial Loss Factor	.00128
Transverse Loss Factor	.0110
Shear Loss Factor	.0110
Mass Density	1.52 gm/cc (.000142 #sec <sup>2</sup> /INA)

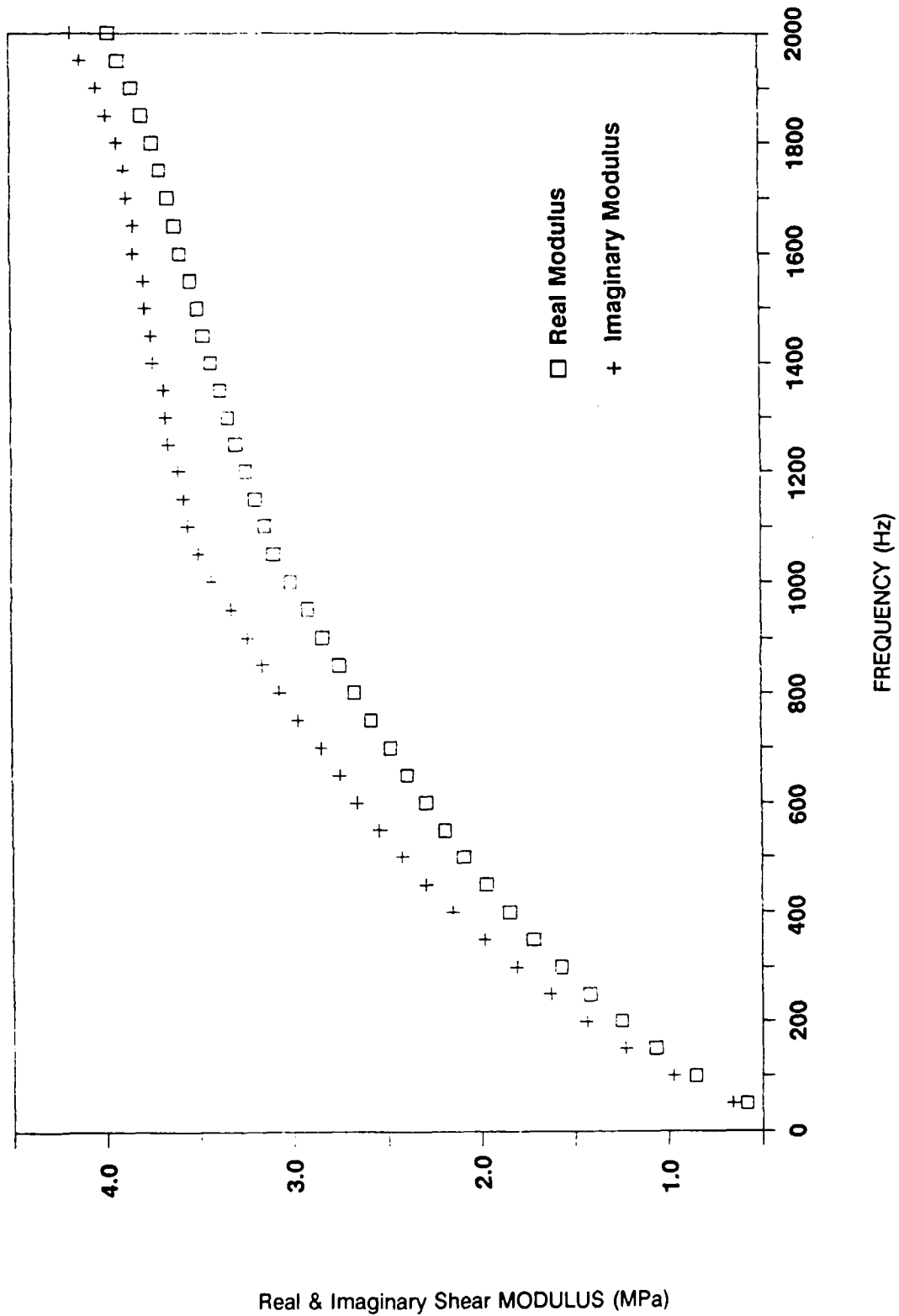


Figure 3. Material Properties Of Scotchdamp SJ 2015 X, Type 112 @ 20°C.

The notation used to specify the structural arrangement of the damped plates is identical to that used for laminations of advanced composites except for the addition of the symbol  $d$  which will indicate the presence of a damping layer. For instance, the baseline structure for this study, so called because it does not include stress coupling or compliant layering effects, is designated  $0_6/d/0_6$ .

#### 4.2 Numerical Results

The first analysis will examine structures with layups of  $0_4/\theta_2/d/\theta_2/0_4$  and  $0_4/\theta_2/d/-\theta_2/0_4$  where the layer orientation angle  $\theta$  is varied between 0 and 90 degrees. The Forced Mode Method is used to compute the loss factors of the first three bending modes of these structures. Plots of the results are shown in Figures 4 and 5. The plots show that for this structure the stress coupling and compliant layering have no effect on the loss factor of the fundamental mode but that these conditions lead to increases in damping in the two higher modes. Also, it is seen that even though stress coupling vanishes at  $\theta=90$  degrees, the highest loss factors are achieved at this orientation. Thus the use of compliant inner layering appears to have more of an effect on damping than stress coupling. Therefore, the rest of the analyses presented here will consider laminated designs without stress coupling. In addition the analyses will also be limited to the study of beams since the second in-plane dimension is no longer needed in the absence of stress coupled lay-ups. (Note that in other structural designs stress coupling may prove to have a greater role in damping. Also note that most of the increase in damping is reached by  $\theta=60$  degrees. This fact may have importance in the fabrication of damped structure.)

Figure 6 shows the loss factors of four different damped beams for the first five bending modes of vibration. Here it is seen that there is little or no gain in damping for the fundamental mode but that in the higher modes the compliant inner layer laminates have significantly greater loss factors. (The matching of natural frequencies of the plates indicates that the gain in damping is not due to changing material properties).

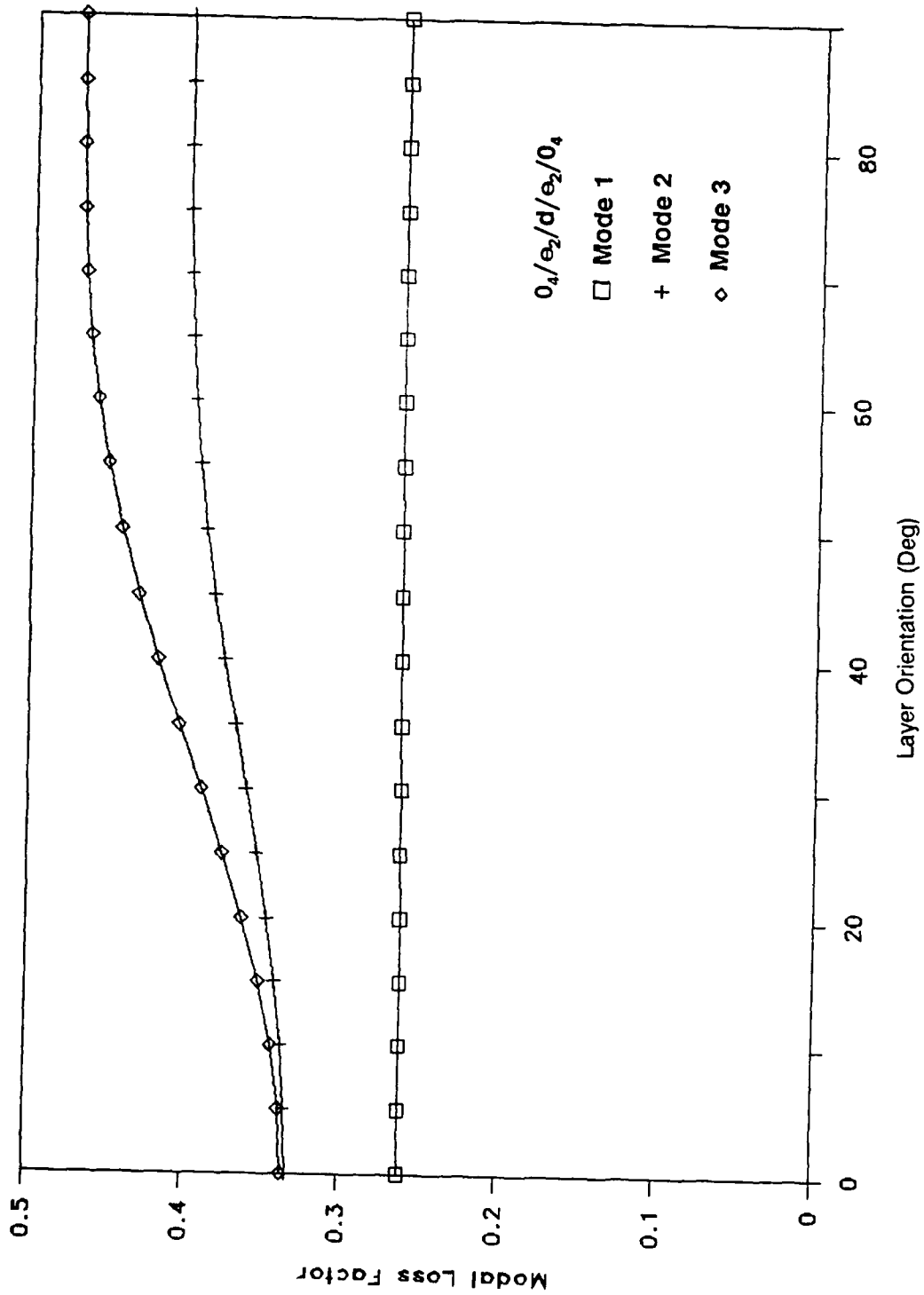


Figure 4. Modal Damping for Bending Modes 1 To 3.

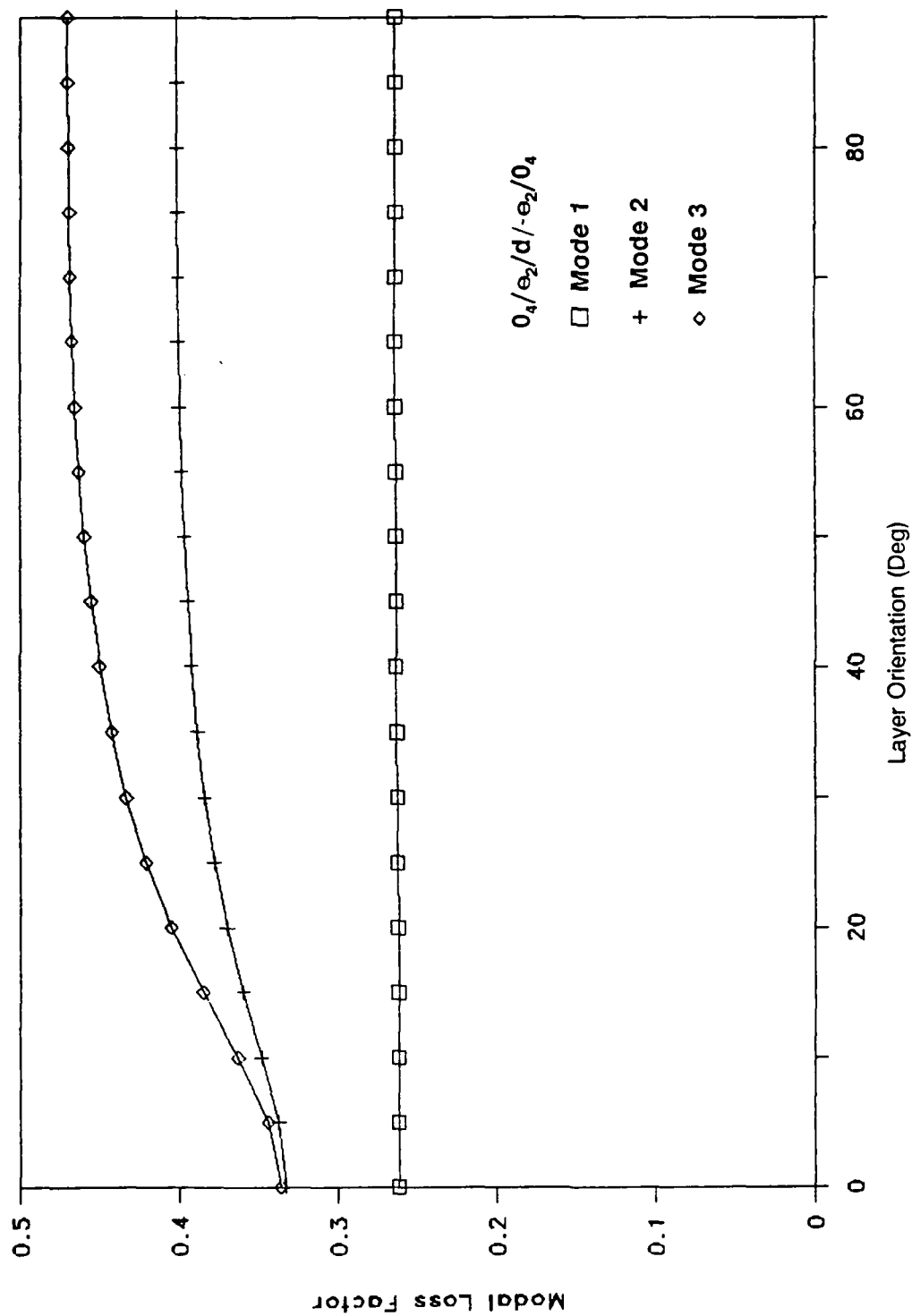


Figure 5. Modal Damping For Bending Modes 1 To 3.

The ineffectiveness of the compliant layering in the fundamental mode is attributed to the particular mix of design variables. Later in the text (Table 2), a design is shown that improves the damping in the fundamental mode but only by resorting to commercially unavailable ply thicknesses. In other design situations the variables (dimensions, material properties, etc.) may be such that improvements in performance can be found across the spectrum.

The goal of a damping design is to reduce resonant stresses and displacements. This is achieved by increasing the structural loss factor which in the laminated designs is accomplished by sacrificing static stiffness (i.e. through the use of 90 degree layer orientations). It is necessary then to verify that the structural response actually decreases in the highly damped but more flexible laminated designs. To analytically test the response, the structures are subjected to forcing functions that approximately excite the resonant response (the approximation is introduced by not accounting for the negligible in-plane and moment components of the load vector that are required by the Forced Mode method for a strict proportionality to the inertia loading). Figure 7 shows the result of this computation where the amplitude of the transverse displacements have been normalized with respect to the modal response of the baseline plate. Except for the fundamental mode where virtually no improvement is achieved, the analysis predicts reduced resonant responses.

The optimal design for vibration resistance is determined through a balance of inertial, stiffness and damping properties. For a given modal excitation, the baseline structure has a unique optimal configuration. But, since the damping material properties are frequency dependent, the optimal design at one mode of response does not necessarily imply an efficient structure over the rest of the spectrum. In making comparisons between the response of the laminated designs and of the baseline structure, there is the concern that the baseline structure is not in an optimal modal configuration. To test this concern, analysis is performed to establish the optimal baseline design for each mode of response. (Note that the ability to actually build an optimal design is limited by the commercial availability of ply thicknesses. The analysis is performed here for the academic reason of establishing the efficacy of the new design

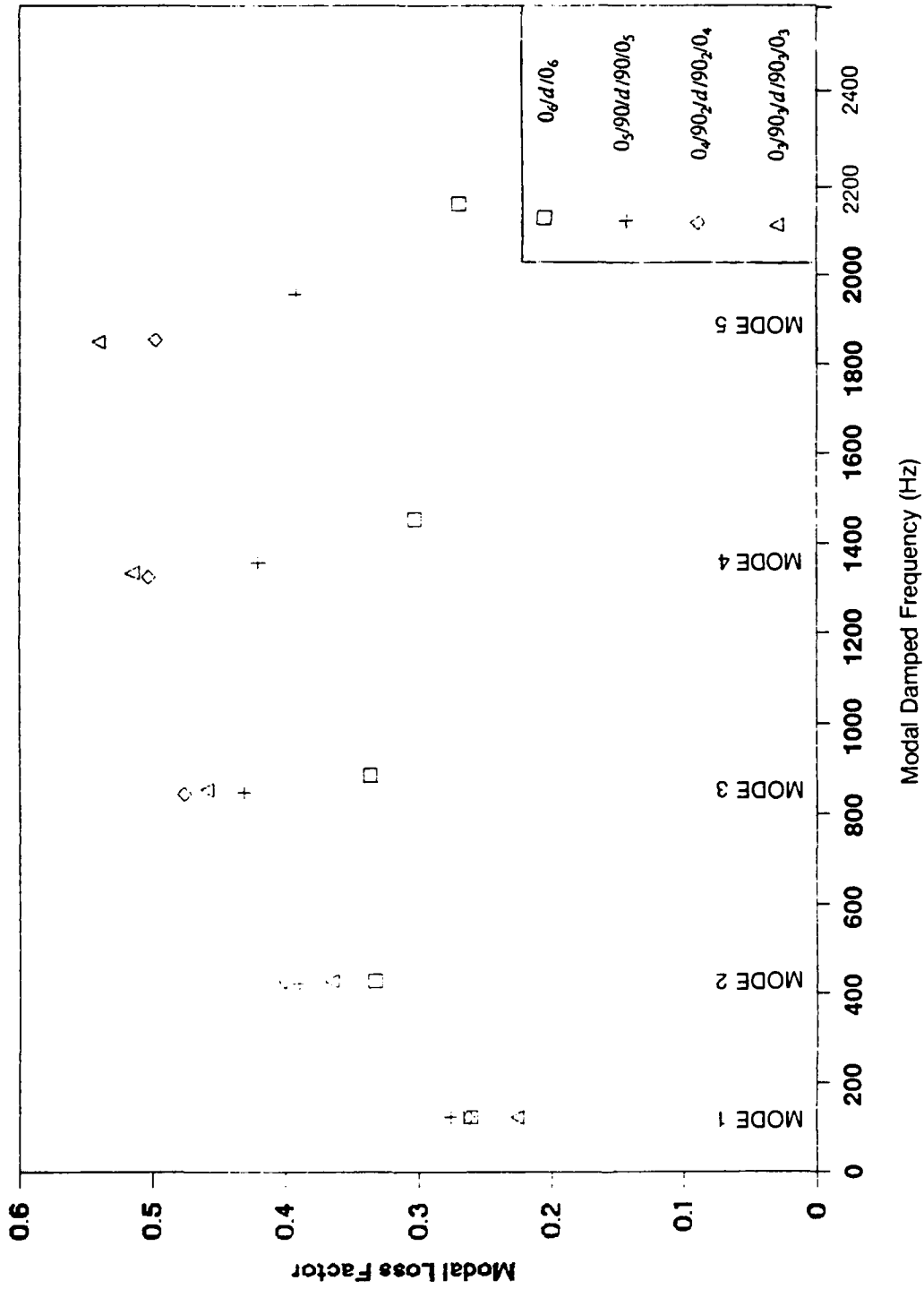


Figure 6. Modal Damping For Bending Modes 1 To 5.



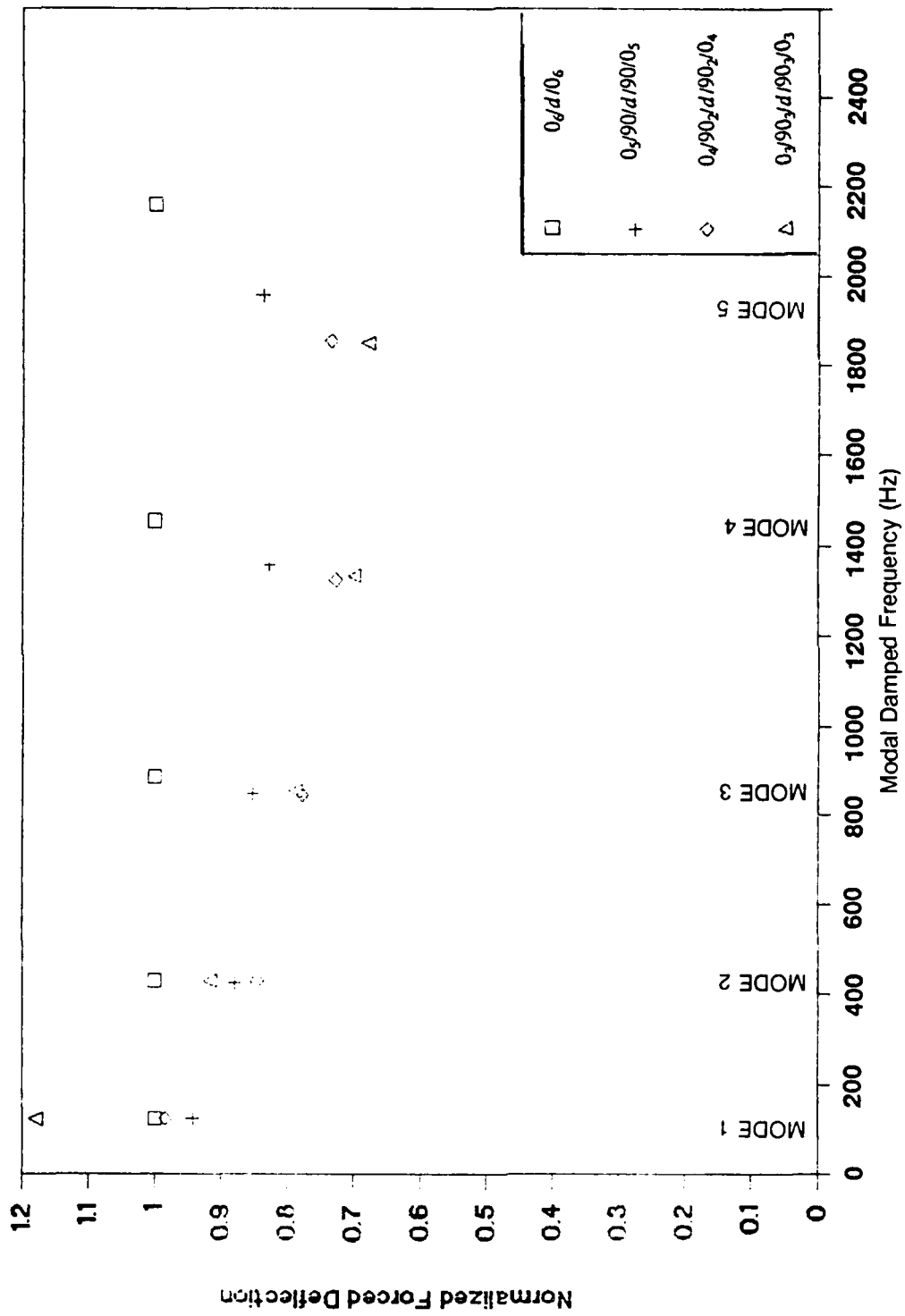


Figure 7. Forced Center Deflection For Bending Modes 1 To 5.

approach.) The overall thickness of the plate remains fixed at 2.17 mm. Given this constraint, the thicknesses of the damping and stiffness layers are varied to determine the optimal configuration. Once an optimal design is determined for the baseline structure, the compliant layered designs are optimized by keeping the thickness of the damping layer constant while varying the thicknesses of the 0 degree layers and 90 degree layers. The results of this analysis are shown in Table 2 where it is seen that for each mode of response a laminated design is found that is superior to the baseline design in increasing the loss factor and reducing the resonant response.

The controlling parameter in increasing the damping in the compliant layered designs is the extensional modulus of the compliant layers. This is seen in Figure 8 where the modulus of the inner layers is varied parametrically as a percentage of the modulus of the outer layers. The loss factor directly increases with decreasing modulus. This modulus also controls the phase lag between the damping layer rotation ( $\alpha_1^D$ ) and the other displacement degrees of freedom (which respond approximately in-phase). Figure 9 shows that this phase lag increases with decreasing modulus. This means that as the beam passes through it's static equilibrium position, the face sheets are increasingly displaced longitudinally with respect to one another as the compliant layer modulus decreases.

Table 2. Optimized Modal Designs

Mode	Type (1)	$t^d/t$	$t^1/t$	$t^2/t$	Loss Factor	Displacement (2)
1	B	6.5	0.0	93.5	.311	1.00
	C	6.5	18.5	75.0	.341	.80
2	B	3.2	0.0	96.8	.296	1.00
	C	3.2	23.1	73.7	.332	.76
3	B	2.3	0.0	97.7	.294	1.00
	C	2.3	27.7	70.0	.337	.72
4	B	1.4	0.0	98.6	.263	1.00
	C	1.4	23.1	75.5	.300	.77

(1) Structural design;

B = Optimized baseline design

C = Optimized compliant layer design

(2) The transverse displacement is normalized with respect to the modal response of the baseline plate

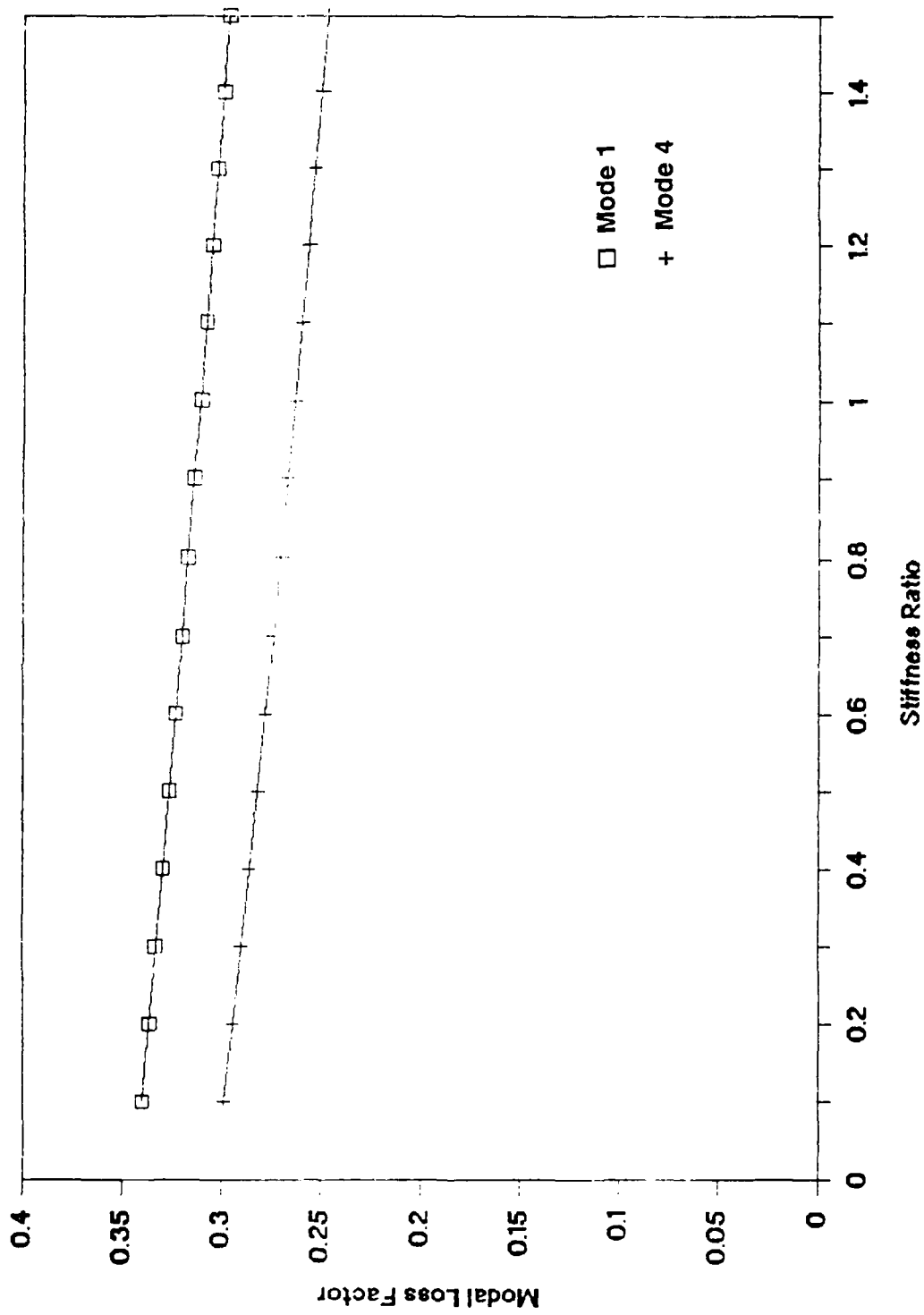


Figure 8. Modal Damping Vs The Modulus Of The Compliant Layer.

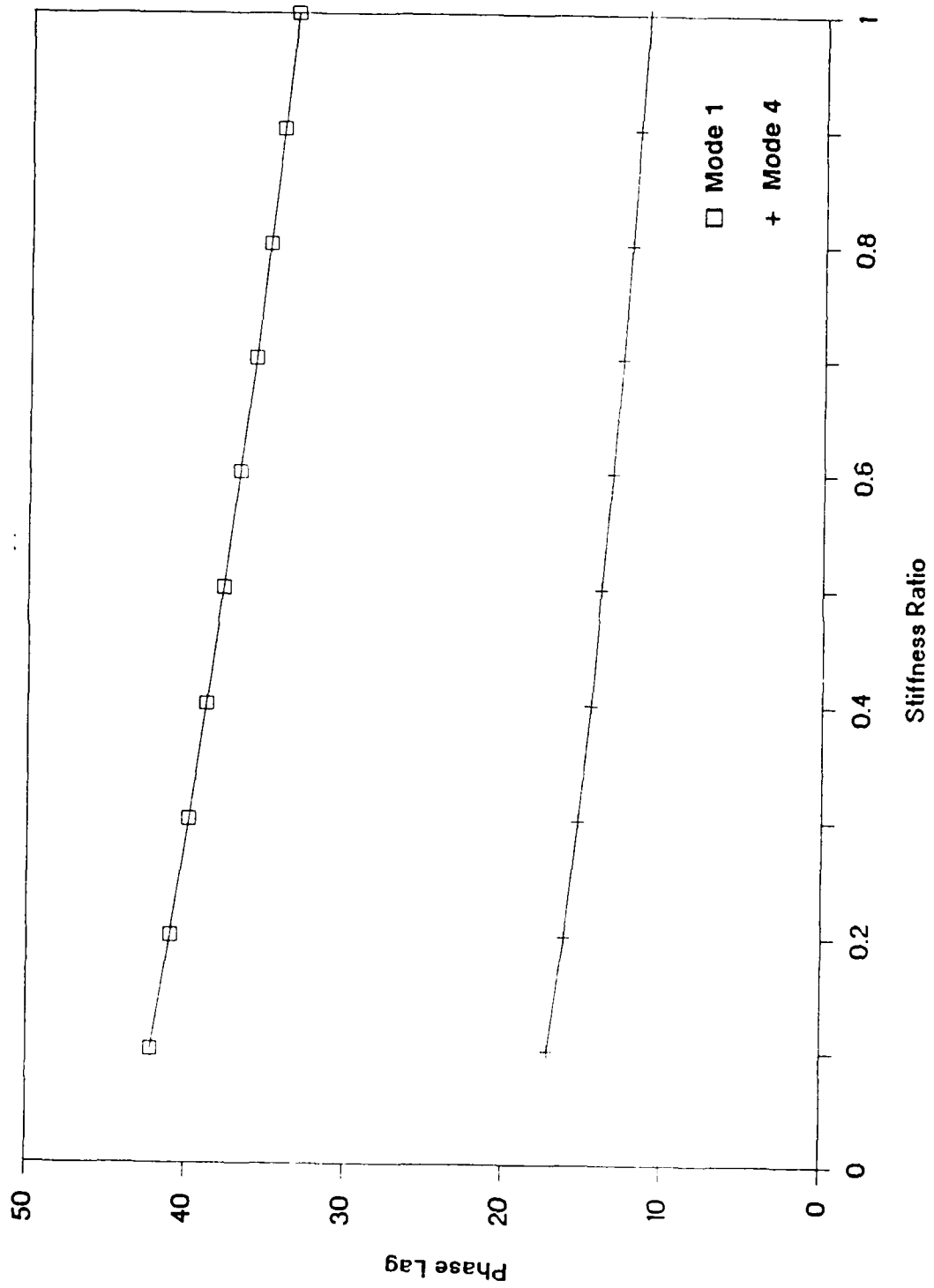


Figure 9. The Phase Lag Of The Core Rotation Vs The Modulus Of The Compliant Layer.

**NADC-90066-60**

THIS PAGE INTENTIONALLY LEFT BLANK

## 5.0 Conclusions

In order to examine the use of anisotropy and lamination in damped plates a structural theory was developed and applied to a simple but representative structural system. The analytical study revealed that compliant layering can increase the efficiency of damping designs.

Compliant layering, which is the replacement of face sheet material with a less stiff material at the interface of the face sheets and the damping layer, affects the dynamic response of the plate through the alteration of stiffness properties. Compliant layering reduces the face sheet axial stiffness without altering the overall structural bending stiffness. This creates a mechanism for increasing the rate of shearing in the damping material by increasing the relative longitudinal displacements of the face sheets. The shearing rate and the associated energy dissipation were found to increase as the modulus of the compliant layer was reduced. However, there is a limitation to this process since the stiffness of the compliant layer must be high enough to confine the shear deformation to the damping layer.

Compliant layering can also be used to reduce the weight of damped structures since compliant materials are generally less massive than stiff materials. For instance, metallic face sheets that incorporate a glass-epoxy compliant layer can have improved dynamic resistance at a reduction in weight. This same effect can be achieved by merely removing some of the material on the inner side of the face sheets through grooving, waffling or scoring this surface.

Compliant layering introduces challenges to the fabrication process since it involves either the mating of dissimilar materials or the unbalancing of quasi-isotropic laminates. Also, there will be additional steps in the laminate fabrication which will add to the cost of building these components. Nevertheless, depending upon the total cost of construction, compliant layering offers an important design option in the use of damped bending elements.

**NADC-90066-60**

THIS PAGE INTENTIONALLY LEFT BLANK



**6.0 References**

1. Soovere, J., and Drake, M. L., "Aerospace Structures Technology Damping Design Guide," AFWAL-TR-84-3089, December 1985.
2. Nashif, A. D., Jones, D. I. G., and Henderson, J. P., "Vibration Damping," John Wiley and Sons, New York, 1985.
3. Drake, M. L., "Passive Damping Impact on Air Force System Maintenance Costs," in The Role of Damping in Vibration and Noise Control, ASME Publication DE-Vol. 5, 1987, pp. 75-80.
4. Vacca, S. N., "Demonstration of Damped Structure for Increased Supportability and Reliability," in The Role of Damping in Vibration and Noise Control, ASME Publication DE-Vol. 5, 1987, pp. 81-87.
5. Kress, G., "Improving Single-Constraining Layer Damping Treatment by Sectioning the Constraining Layer," in The Role of Damping in Vibration and Noise Control, ASME Publication DE-Vol. 5, 1987, pp. 41-48.
6. Miles, R. N. and Reinhall, P. G., "An Analytical Model for the Vibration of Laminated Beams Including the Effects of Both Shear and Thickness Deformation in the Adhesive Layer," Journal of Vibration, Acoustics, Stress, and Reliability in Design, Vol. 108, January 1986, pp. 56-64.
7. Douglas, B. E., "Compressional Damping in Three-Layer Beams Incorporating Nearly Incompressible Viscoelastic Cores," Journal of Sound and Vibration, Vol. 104 (2), 1986, pp. 343-347.
8. Mukhopadhyay, A. K. and Kingsbury, H. B., "On the Dynamic Response of Rectangular Sandwich Plate with Viscoelastic Core and Generally Orthotropic Facings," Journal of Sound and Vibration, Vol. 47 (3), 1976, pp. 347-358.
9. Barrett, D. J., "Optimization of Damping Properties of Structural Components," Final Report to NSF, Grant No. ISI-8560810, July 1986.
10. Barrett, D. J., "A Design for Improving the Structural Damping Properties of Axial Members," in the Proceedings of Damping '89 (To be published as an AFWAL Technical Report).

11. Mead, D. J. and Markus, S., "The Forced Vibration of a Three Layer Damped Sandwich Beam with Arbitrary Boundary Conditions," Journal of Sound and Vibration, Vol. 10 (2), 1969, pp. 163-175.

## Appendix A - Matrix Elements

The elements of the mass matrix  $[M]$  are

$$[M] = \begin{bmatrix} M & 0 & 0 & I_1^D & 0 & I_1^T & 0 & I_1^B & 0 \\ 0 & M & 0 & 0 & I_1^D & 0 & I_1^T & 0 & I_1^B \\ 0 & 0 & M & 0 & 0 & 0 & 0 & 0 & 0 \\ I_1^D & 0 & 0 & I_2^D & 0 & I_2^T & 0 & I_2^B & 0 \\ 0 & I_1^D & 0 & 0 & I_2^D & 0 & I_2^T & 0 & I_2^B \\ I_1^T & 0 & 0 & I_2^T & 0 & I_3^T & 0 & 0 & 0 \\ 0 & I_1^T & 0 & 0 & I_2^T & 0 & I_3^T & 0 & 0 \\ I_1^B & 0 & 0 & I_2^B & 0 & 0 & 0 & I_3^B & 0 \\ 0 & I_1^B & 0 & 0 & I_2^B & 0 & 0 & 0 & I_3^B \end{bmatrix}$$

The elements of the operator matrix  $[D]$  are

$$[D] = \begin{bmatrix} D_{11}d_{,11} & D_{12}d_{,11} & 0 & D_{14}d_{,11} & D_{15}d_{,11} & D_{16}d_{,11} & D_{17}d_{,11} & D_{18}d_{,11} & D_{19}d_{,11} \\ D_{21}d_{,11} & D_{22}d_{,11} & 0 & D_{24}d_{,11} & D_{25}d_{,11} & D_{26}d_{,11} & D_{27}d_{,11} & D_{28}d_{,11} & D_{29}d_{,11} \\ 0 & 0 & D_{33}d_{,11} & D_{34}d_{,11} & 0 & D_{36}d_{,11} & D_{37}d_{,11} & D_{38}d_{,11} & D_{39}d_{,11} \\ D_{41}d_{,11} & D_{42}d_{,11} & D_{43}d_{,11} & D_{44}d_{,11} + D_{442} & D_{45}d_{,11} & D_{46}d_{,11} & D_{47}d_{,11} & D_{48}d_{,11} & D_{49}d_{,11} \\ D_{51}d_{,11} & D_{52}d_{,11} & 0 & D_{54}d_{,11} & D_{55}d_{,11} + D_{552} & D_{56}d_{,11} & D_{57}d_{,11} & D_{58}d_{,11} & D_{59}d_{,11} \\ D_{61}d_{,11} & D_{62}d_{,11} & D_{63}d_{,11} & D_{64}d_{,11} & D_{65}d_{,11} & D_{66}d_{,11} + D_{662} & D_{67}d_{,11} + D_{672} & 0 & 0 \\ D_{71}d_{,11} & D_{72}d_{,11} & D_{73}d_{,11} & D_{74}d_{,11} & D_{75}d_{,11} & D_{76}d_{,11} + D_{762} & D_{77}d_{,11} + D_{772} & 0 & 0 \\ D_{81}d_{,11} & D_{82}d_{,11} & D_{83}d_{,11} & D_{84}d_{,11} & D_{85}d_{,11} & 0 & 0 & D_{88}d_{,11} + D_{882} & D_{89}d_{,11} + D_{892} \\ D_{91}d_{,11} & D_{92}d_{,11} & D_{93}d_{,11} & D_{94}d_{,11} & D_{95}d_{,11} & 0 & 0 & D_{98}d_{,11} + D_{982} & D_{99}d_{,11} + D_{992} \end{bmatrix}$$

where the  $D_{ij}$  are

$$D_{11} = -(A_{111}^T + A_{111}^B)$$

$$D_{12} = D_{21} = -(A_{112}^T + A_{112}^B)$$

$$D_{15} = D_{51} = \frac{1}{2} t^D (-A_{112}^T + A_{112}^B)$$

$$D_{17} = D_{71} = (\frac{1}{2} t^D A_{112}^T - B_{112}^T)$$

$$D_{19} = D_{91} = -(\frac{1}{2} t^D A_{112}^B + B_{112}^B)$$

$$D_{22} = -(A_{1212}^T + A_{1212}^B + G t^D)$$

$$D_{24} = D_{42} = \frac{1}{2} t^D (-A_{112}^T + A_{112}^B)$$

$$D_{26} = D_{62} = (\frac{1}{2} t^D A_{112}^T - B_{112}^T)$$

$$D_{28} = D_{82} = -(\frac{1}{2} t^D A_{112}^B + B_{112}^B)$$

$$D_{33} = -(E_{11}^T + E_{11}^B + G t^D)$$

$$D_{34} = -D_{43} = -G t^D$$

$$D_{37} = -D_{73} = -E_{12}^T$$

$$D_{39} = -D_{93} = -E_{12}^B$$

$$D_{441} = -(\frac{1}{2} t^D)^2 (A_{1111}^T + A_{1111}^B)$$

$$D_{45} = D_{54} = -(\frac{1}{2} t^D)^2 (A_{1112}^T + A_{1112}^B)$$

$$D_{47} = D_{74} = \frac{1}{2} t^D (\frac{1}{2} t^D A_{1112}^T - B_{1112}^T)$$

$$D_{49} = D_{94} = \frac{1}{2} t^D (\frac{1}{2} t^D A_{1112}^B + B_{1112}^B)$$

$$D_{551} = -(\frac{1}{2} t^D)^2 (A_{1212}^T + A_{1212}^B) - \frac{G (t^D)^3}{12}$$

$$D_{56} = D_{65} = \frac{1}{2} t^D (\frac{1}{2} t^D A_{1112}^T - B_{1112}^T)$$

$$D_{58} = D_{85} = \frac{1}{2} t^D (\frac{1}{2} t^D A_{1112}^B + B_{1112}^B)$$

$$D_{661} = (\frac{1}{2} t^D)^2 A_{1111}^T + t^D B_{1111}^T - D_{1111}^T$$

$$D_{14} = D_{41} = \frac{1}{2} t^D (-A_{1111}^T + A_{1111}^B)$$

$$D_{16} = D_{61} = (\frac{1}{2} t^D A_{1111}^T - B_{1111}^T)$$

$$D_{18} = D_{81} = -(\frac{1}{2} t^D A_{1111}^B + B_{1111}^B)$$

$$D_{25} = D_{52} = \frac{1}{2} t^D (-A_{1212}^T + A_{1212}^B)$$

$$D_{27} = D_{72} = (\frac{1}{2} t^D A_{1212}^T - B_{1212}^T)$$

$$D_{29} = D_{92} = -(\frac{1}{2} t^D A_{1212}^B + B_{1212}^B)$$

$$D_{36} = -D_{63} = -E_{11}^T$$

$$D_{38} = -D_{83} = -E_{11}^B$$

$$D_{442} = G t^D$$

$$D_{46} = D_{64} = \frac{1}{2} t^D (\frac{1}{2} t^D A_{1111}^T - B_{1111}^T)$$

$$D_{48} = D_{84} = \frac{1}{2} t^D (\frac{1}{2} t^D A_{1111}^B + B_{1111}^B)$$

$$D_{552} = G t^D$$

$$D_{57} = D_{75} = \frac{1}{2} t^D (\frac{1}{2} t^D A_{1212}^T - B_{1212}^T)$$

$$D_{59} = D_{95} = \frac{1}{2} t^D (\frac{1}{2} t^D A_{1212}^B + B_{1212}^B)$$

$$D_{662} = E_{11}^T$$

$$D_{671} = D_{761} = -\left(\frac{1}{2}t^D\right)^2 A_{1112}^T + t^D B_{1112}^T - D_{1112}^T \quad D_{672} = D_{762} = E_{12}^T$$

$$D_{771} = -\left(\frac{1}{2}t^D\right)^2 A_{1212}^T + t^D B_{1212}^T - D_{1212}^T \quad D_{772} = E_{22}^T$$

$$D_{881} = -\left(\frac{1}{2}t^D\right)^2 A_{1111}^B - t^D B_{1111}^B - D_{1111}^B \quad D_{882} = E_{11}^B$$

$$D_{891} = D_{981} = -\left(\frac{1}{2}t^D\right)^2 A_{1112}^B - t^D B_{1112}^B - D_{1112}^B \quad D_{892} = D_{982} = E_{12}^B$$

$$D_{991} = -\left(\frac{1}{2}t^D\right)^2 A_{1212}^B - t^D B_{1212}^B - D_{1212}^B \quad D_{992} = E_{22}^B$$

and where  $d_{,1}$  and  $d_{,11}$  denote the first and second order differentiation with respect to the spatial variable  $x_1$ .

The displacement degree of freedom vector is

$$[u] = \begin{bmatrix} u_1^0 \\ u_2^0 \\ u_3^0 \\ \alpha_1^D \\ \alpha_2^D \\ \alpha_1^T \\ \alpha_2^T \\ \alpha_1^B \\ \alpha_2^B \end{bmatrix}$$

The load vector is

$$[P] = \begin{bmatrix} P_1 \\ P_2 \\ P_3 \\ 0 \\ 0 \\ 0 \\ 0 \\ 0 \\ 0 \end{bmatrix}$$

The Fourier displacement coefficient vector is

$$[U^m] = \begin{bmatrix} U_1^m \\ U_2^m \\ U_3^m \\ A_1^{mD} \\ A_2^{mD} \\ A_1^{mT} \\ A_2^{mT} \\ A_1^{mB} \\ A_2^{mB} \end{bmatrix}$$

The Fourier loading coefficient vector is

$$[P^m] = \begin{bmatrix} P_1^m \\ P_2^m \\ P_3^m \\ 0 \\ 0 \\ 0 \\ 0 \\ 0 \\ 0 \end{bmatrix}$$

The elements of the symmetric  $[B_m]$  matrix are

$$[B_m] = \begin{bmatrix} B_m^{11} & B_m^{12} & 0 & B_m^{14} & B_m^{15} & B_m^{16} & B_m^{17} & B_m^{18} & B_m^{19} \\ B_m^{21} & B_m^{22} & 0 & B_m^{24} & B_m^{25} & B_m^{26} & B_m^{27} & B_m^{28} & B_m^{29} \\ 0 & 0 & B_m^{33} & B_m^{34} & 0 & B_m^{36} & B_m^{37} & B_m^{38} & B_m^{39} \\ B_m^{41} & B_m^{42} & B_m^{43} & B_m^{44} & B_m^{45} & B_m^{46} & B_m^{47} & B_m^{48} & B_m^{49} \\ B_m^{51} & B_m^{52} & 0 & B_m^{54} & B_m^{55} & B_m^{56} & B_m^{57} & B_m^{58} & B_m^{59} \\ B_m^{61} & B_m^{62} & B_m^{63} & B_m^{64} & B_m^{65} & B_m^{66} & B_m^{67} & 0 & 0 \\ B_m^{71} & B_m^{72} & B_m^{73} & B_m^{74} & B_m^{75} & B_m^{76} & B_m^{77} & 0 & 0 \\ B_m^{81} & B_m^{82} & B_m^{83} & B_m^{84} & B_m^{85} & 0 & 0 & B_m^{88} & B_m^{89} \\ B_m^{91} & B_m^{92} & B_m^{93} & B_m^{94} & B_m^{95} & 0 & 0 & B_m^{98} & B_m^{99} \end{bmatrix}$$

where the  $B_m^{ij}$  are computed from either

$$B_m^{ij} = -D_{ij} \left( \frac{m\pi}{a} \right)^2 \quad i, j \neq 3$$

or

$$-B_m^{i3} = B_m^{3j} = D_{ij} \left( \frac{m\pi}{a} \right)$$

with the exception of the following elements

$$B_m^{33} = -D_{33} \left( \frac{m\pi}{a} \right)^2$$

$$B_m^{44} = -D_{441} \left( \frac{m\pi}{a} \right)^2 + D_{442}$$

$$B_m^{55} = -D_{551} \left( \frac{m\pi}{a} \right)^2 + D_{552}$$

$$B_m^{66} = -D_{661} \left( \frac{m\pi}{a} \right)^2 + D_{662}$$

$$B_m^{67} = -D_{671} \left( \frac{m\pi}{a} \right)^2 + D_{672}$$

$$B_m^{77} = -D_{771} \left( \frac{m\pi}{a} \right)^2 + D_{772}$$

$$B_m^{88} = -D_{881} \left( \frac{m\pi}{a} \right)^2 + D_{882}$$

$$B_m^{89} = -D_{891} \left( \frac{m\pi}{a} \right)^2 + D_{892}$$

$$B_m^{99} = -D_{991} \left( \frac{m\pi}{a} \right)^2 + D_{992}$$



DISTRIBUTION LIST (Continued)  
Report No. NADC-90066-60

	No. of Copies
<b>Pennsylvania State University</b> <b>Attn: Dr. T. Hahn</b> <b>Dept. Engineering Science &amp; Mechanics</b> <b>227 Hammond Building</b> <b>University Park, PA 16802</b>	
<b>Purdue University</b> ..... <b>Attn: Dr. C. T. Sun</b> <b>School of Aeronautics &amp; Astronautics</b> <b>West Lafayette, IN 47907</b>	1
<b>Rockwell International</b> ..... <b>Attn: Mr. M. Schweiger</b> <b>Columbus, OH 43216</b>	1
<b>Tuskegee University</b> ..... <b>Attn: Vascar G. Harris, Dean</b> <b>School of Engineering and Architecture</b> <b>Tuskegee, AL 36088</b>	1
<b>Teledyne Ryan Aeronautical Company</b> ..... <b>Attn: Mr. J. Hill</b> <b>2701 N. Harbor Dr., MS 340H, Dept. 194</b> <b>P. O. Box 80311</b> <b>San Diego, CA 92138-9012</b>	1
<b>Villanova University</b> ..... <b>Attn: Dr. P. V. McLaughlin</b> <b>Department of Mechanical Engineering</b> <b>Villanova, PA 19085</b>	1
<b>Virginia Polytechnic Institute</b> ..... <b>Attn: Dr. K. Reifsnider</b> <b>Materials Response Group</b> <b>Blacksburg, VA 24061</b>	1
<b>University of Wyoming</b> ..... <b>Attn: Dr. Donald Adams</b> <b>Professor of Mechanical Engineering</b> <b>Composite Material Research Group</b> <b>P. O. Box 3295</b> <b>Laramie, WY 82071</b>	1
<b>Naval Air Development Center</b> ..... <b>Warminster, PA 18974-5000</b> <b>( 2 copies for Code 8131)</b> <b>(20 copies for Code 6042)</b>	22

DISTRIBUTION LIST (Continued)  
Report No. NADC-90066-60

	No. of Copies
Lockheed Aeronautical Systems Company . . . . .	1
Attn: Mr. A. M. James	
Advanced Structures Technology Dept.	
Dept. 76-23, Bldg. 63, Plt. A-1	
P. O. Box 551	
Burbank, CA 91520	
Lockheed-Georgia Co. . . . .	1
Attn: Technical Information	
Dept. 72-34, Zone 26	
Marietta, GA 30063	
Lockheed-Missile & Space Co. . . . .	1
Attn: Mr. J. A. Bailie - Dept. 81-12	
Bldg. 154	
P. O. Box 504	
1111 Lockheed Way	
Sunnyvale, CA 94088	
LTV Aerospace and Defense Co. . . . .	1
Vought Missiles and Advanced Programs Division	
Attn: Mr. R. Knight - MS-TH-83	
P. O. Box 65003	
Dallas, TX 75265-0003	
Massachusetts Institute of Technology . . . . .	1
Attn: Dr. P. A. Lagace	
Dept. of Aeronautics and Astronautics	
Technology Laboratory for Advanced Composites	
77 Massachusetts Avenue	
Cambridge, MA 02139	
McDonnell Douglas Corporation . . . . .	1
McDonnell Aircraft Company	
Attn: Dr. Michael E. Renieri	
MS 370	
Dept 337, Bldg. 66	
P. O. Box 516	
St. Louis, MO 63166	
University of Oklahoma . . . . .	1
Attn: Dr. C. W. Bert	
School of Aeronautics, Mechanical, Nuclear Engineering	
Norman, OK 73019	

DISTRIBUTION LIST (Continued)  
Report No. NADC-90066-60

	No. of Copies
Drexel University . . . . .	1
Attn: Dr. Frank Ko	
Fibrous Materials and Research Lab	
32nd and Chestnut Street	
Philadelphia, PA 19104	
E. I. DuPont Company . . . . .	1
Attn: Mr. V. L. Bertarelli	
Chestnut Run Location, CR701	
Wilmington, DE 19898	
General Dynamics Corporation . . . . .	1
Fort Worth Division	
Attn: Composite Structures Eng. Dept.	
P. O. Box 748	
Fort Worth, TX 76101	
General Electric Co. . . . .	1
Space Systems Division	
Attn: Mr. A. Garber, MS M4018/BL100	
P. O. Box 8555	
Philadelphia, PA 19101	
General Electric Co. . . . .	1
Attn: Mr. C. Zweben - MS M4018/BL 100	
P. O. Box 8555	
Philadelphia, PA 19101	
Hercules Aerospace Division . . . . .	1
Attn: Mr. D. Hug	
P. O. Box 210	
Rocket Center, WV 26726	
HITCO . . . . .	1
Attn: Mr. N. Myers	
1600 West 135th Street	
Gardena, CA 90249	
Lehigh University . . . . .	1
Attn: Dr. G. C. Sih	
Institute of Fracture and	
Solid Mechanics	
Bethlehem, PA 18015	

DISTRIBUTION LIST (Continued)  
Report No. NADC-90066-60

	No. of Copies
University of California . . . . . Attn: Professor Lawrence Rehfield Department of Mechanical Engineering Davis, CA 95616	1
University of Dayton Research Institute . . . . . Attn: Dr. J. Gallagher 300 College Park Avenue Dayton, OH 45469	1
University of Delaware . . . . . Attn: Dr. R. B. Pipes Mechanics & Aerospace Eng. Dept. Evans Hall Newark, DE 19711	1
University of Delaware . . . . . Attn: Dr. J. R. Vinson Mechanics & Aerospace Eng. Dept. Evans Hall Newark, DE. 19711	1
University of Delaware . . . . . Attn: Dr. D. Wilkins Mechanics & Aerospace Eng. Dept. Evans Hall Newark, DE. 19711	1
Department of Transportation . . . . . Attn: Dr. Pin Tong, DTS 76, TSC Kendall Square Cambridge, MA 02142	1
Drexel University . . . . . Attn: Dr. P. C. Chou Mechanical Engineering Dept. 32nd and Chestnut Street Philadelphia, PA 19104	1
Drexel University . . . . . Attn: Dr. A. S. D. Wang Mechanical Engineering Dept. 32nd and Chestnut Street Philadelphia, PA 19104	1

DISTRIBUTION LIST (Continued)  
Report No. NADC-90066-60

	No. of Copies
Administrator ..... National Aeronautics and Space Adm. Langley Research Center Attn: Mr. W. T. Freeman, Mail Code 243 Hampton, VA 23365-5225	1
Federal Aviation Administration ..... Attn: Mr. J. R. Soderquist, AW 103 800 Independence Avenue, SW Washington D. C. 20591	1
Federal Aviation Administration ..... Attn: L. Neri, Code ACT-330 Technical Center Atlantic City, NJ 08405	1
Administrator ..... Defense Technical Information Center Bldg. #5, Cameron Station Alexandria, VA 22314	2
Alcoa Defense Systems Corp. .... Attn: Mr. D. Myers 16761 Via delCampo Court San Diego, CA 92127	1
Anamet Laboratories, Inc. .... Attn: Dr. Rocky R. Arnold 3400 Industrial Way San Carlos, CA 94077	1
AVCO ..... Attn: Mr. William F. Grant Specialty Materials Division 2 Industrial Avenue Lowell, MA 01851	1
Battelle Memorial Institute ..... Metals and Ceramics Information Center 505 King Avenue Columbus, OH 43201	1
Bell Aerospace Company Attn: Mr. F. M. Anthony, Zone S-69 P. O. Box 1 Buffalo, NY 14240	

DISTRIBUTION LIST (Continued)  
Report No. NADC-90066 60

	No. of Copies
Headquarters ..... National Aeronautics and Space Adm. Attn: Dr. D. Mulville OAST-RM Washington, D.C. 20546	1
Administrator ..... National Aeronautics and Space Adm. Attn: Airframes Branch, FS 120 Washington, D.C. 20546	1
Administrator ..... National Aeronautics and Space Adm. Langley Research Center Attn: C. E. Harris, MS 188E Hampton, VA 23365-5225	1
Administrator ..... National Aeronautics and Space Adm. Langley Research Center Attn: Dr. J. Starnes, MS 190 Hampton, VA 23365-5225	1
Administrator ..... National Aeronautics and Space Adm. Langley Research Center Attn: Dr. M. Mikulus, MS 188A Hampton, VA 23365-5225	1
Administrator ..... National Aeronautics and Space Adm. George C. Marshall Space Flight Center Attn: R. Schwinghamer, S&E-ASTN-M Huntsville, AL 35812	1
Administrator ..... National Aeronautics and Space Adm. Lewis Research Center Attn: Dr. C. Chamis, MS-49-6 21000 Brookpark Rd. Cleveland, OH 44135	1
Administrator ..... National Aeronautics and Space Adm. Lewis Research Center Attn: Mr. Hershberg, MS-49-6 21000 Brookpark Rd. Cleveland, OH 44135	1

DISTRIBUTION LIST (Continued)  
Report No. NADC-90066-60

	No. of Copies
Commanding Officer . . . . .	1
Wright Research and Development Center	
Attn: MLBM/Dr. J. Whitney	
Wright Patterson Air Force Base	
OH 45433-6533	
Commanding Officer . . . . .	1
Wright Research and Development Center	
Attn: MLSE/J. Reinhart	
Wright Patterson Air Force Base	
OH 45433-6533	
Commanding Officer . . . . .	1
Wright Research and Development Center	
Attn: MLSE/F. Fecheck	
Wright Patterson Air Force Base	
OH 45433-6533	
Commanding Officer . . . . .	1
U.S. Army Aviation Applied Technology Directorate	
Attn: G. McAllister USAF.TL, (AVRADCOM)	
Ft. Eustis, VA 23604-5418	
Commanding Officer . . . . .	1
U.S. Army Material & Mechanical Research Center	
Attn: D. Oplinger, SLCMT-MS	
Watertown, MA 02172-0001	
Commanding Officer . . . . .	1
U. S. Army R&T Laboratory (AVRADCOM)	
Attn: F. Immen, DAVDL-AS-MS 207-5	
Ames Research Center	
Moffet Field, CA 94035	
Commanding Officer . . . . .	1
Picatinny Arsenal	
PLASTEC	
Attn: H. Pebly	
Dover, NJ 07801	
Commanding Officer . . . . .	1
Picatinny Arsenal	
PLASTEC	
Attn: Librarian, Code DRDAR-SCM-O	
Bldg. 351N	
Dover, NJ 07801	

DISTRIBUTION LIST (Continued)  
Report No. NADC-90066-60

	No. of Copies
Department of the Air Force .....	1
Attn: Dr. J. Amos	
Building 410	
Bolling Air Force Base	
Washington, D.C. 20331	
 Commanding Officer .....	 1
Wright Research and Development Center	
Attn: FIBEC/Dr. G. Sendeckyj	
Wright Patterson Air Force Base	
OH 45433-6553	
 Commanding Officer .....	 1
Wright Research and Development Center	
Attn: FIBA/L. Kelly	
Wright Patterson Air Force Base	
OH 45433-6553	
 Commanding Officer .....	 1
Wright Research and Development Center	
Attn: FIBA/W. Goesch	
Wright Patterson Air Force Base	
OH 45433-6553	
 Commanding Officer .....	 1
Wright Research and Development Center	
Attn: FIBCA/C. Ramsey	
Wright Patterson Air Force Base	
OH 45433-6533	
 Commanding Officer .....	 1
Wright Research and Development Center	
Attn: FIBR/Dr. L. C. Rogers	
Wright Patterson Air Force Base	
OH 45433-6533	
 Commanding Officer .....	 1
Wright Research and Development Center	
Attn: FIBR/H. F. Wolfe	
Wright Patterson Air Force Base	
OH 45433-6533	
 Commanding Officer .....	 1
Wright Research and Development Center	
Attn: MLBM/Mr. M. Knight	
Wright Patterson Air Force Base	
OH 45433-6533	



DISTRIBUTION LIST (Continued)  
Report No. NADC-90066-60

	No. of Copies
Commander ..... United States Naval Academy Attn: Mechanical Engr. Department Annapolis, MD 21402	1
Commander ..... David Taylor Research Center Attn: A. Macander, Code 1720 Bethesda, MD 20084	1
Commander ..... David Taylor Research Center Attn: E. T. Camponeschi, Code 2844 Annapolis, MD 21402	1
Commander ..... David Taylor Research Center Attn: R. Crane, Code 2844 Annapolis, MD 21402	1
Commander ..... David Taylor Research Center Attn: Lori Wall, Code 17202 Bethesda, MD 20084-5000	1
Commander ..... David Taylor Research Center Attn: H. Edelstein, Code 2870 Annapolis, MD 21401	1
Commander ..... Naval Surface Weapons Center Attn: Dr. J. Goff - R-34 White Oak Laboratory Silver Spring, MD 20910	1
Commander ..... Naval Surface Weapons Center Attn: Dr. J. M. Augl 10901 New Hampshire Avenue Silver Spring, MD 20903-5000	1
Department of the Air Force ..... Attn: Dr. M. Salkind Building 410 Bolling Air Force Base Washington, D.C. 20331	1

DISTRIBUTION LIST (Continued)  
Report No. NADC-90066-60

	No. of Copies
Commander . . . . .	1
Naval Air Systems Command	
Attn: AIR-53022	
Washington, D.C. 20361-5300	
 Commander . . . . .	 1
Naval Systems Command	
Attn: T. Momiyama, AIR-931	
Washington, D.C. 20361-9300	
 Commander . . . . .	 1
Naval Air Systems Command	
Attn: G. Seidel, AIR-931B	
Washington, D.C. 20361-9300	
 Commander . . . . .	 1
Naval Sea Systems Command	
Attn: C. Zannis, Sea 05R	
Washington, D.C. 20362	
 Commander . . . . .	 1
U. S. Naval Post Graduate School	
Attn: Professor R. Ball, Code 67BP	
Monterey, CA 93940	
 Commander . . . . .	 1
U. S. Naval Post Graduate School	
Attn: Dr. E. Robert Wood (Code 67)	
Monterey, CA 93940	
 Commander . . . . .	 1
U. S. Naval Post Graduate School	
Attn: Professor M. H. Bank, Code 67BP	
Monterey, CA 93943	
 Commander . . . . .	 1
U. S. Naval Post Graduate School	
Attn: Professor K. Challenger	
Monterey, CA 93943	
 Commander . . . . .	 1
U. S. Naval Post Graduate School	
Attn: Professor Y. S. Shin	
Monterey, CA 93943	

**DISTRIBUTION LIST**  
**Report No. NADC-90066-60**

	No. of Copies
Office of Secretary of Defense .....	1
Attn: P. W. Bzdak	
Weapon Support Improvement	
5203 Leesburg Pike	
Falls Church, VA 22041	
Office of Naval Technology .....	1
Attn: W. King, ONT-212	
800 N. Quincy Street	
Arlington, VA 22217	
Office of Naval Research .....	1
Attn: A. K. Vasudevan, Code 1216	
800 North Quincy Street	
Arlington, VA 22217	
Director .....	1
Naval Research Laboratory	
Attn: Dr. R. Badalian, Code 6380	
4555 Overlook Avenue, SW	
Washington, D.C. 20375	
Director .....	1
Naval Research Laboratory	
Attn: Dr. I. Wolock, Code 383	
4555 Overlook Avenue, SW	
Washington, D.C. 20375-5000	
Office of Naval Research .....	1
Attn: Y. Rajapakse, Code 1132SM	
800 N. Quincy Street	
Arlington, VA 22217	
Commander .....	1
Naval Air Systems Command	
Attn: AIR-530	
Washington, D. C. 20361-5300	
Commander .....	1
Naval Air Systems Command	
Attn: AIR-5302	
Washington, D. C. 20361-5300	
Commander .....	1
Naval Air Systems Command	
Attn: AIR-53201	
Washington, D.C. 20361-5300	

**END  
FILMED**

**DATE:** 5-91

**DTIC**